

# Tail maximal dependence in bivariate models: estimation and applications

Ning Sun<sup>1</sup>, Chen Yang<sup>\*,2</sup>, and Ričardas Zitikis<sup>1,3</sup>

<sup>1</sup>School of Mathematical and Statistical Sciences, Western University, London,  
Ontario N6A 5B7, Canada

<sup>2</sup>Department of Population Health Science and Policy, Icahn School of Medicine at Mount  
Sinai, New York, NY 10029, U.S.A.

<sup>3</sup>Risk and Insurance Studies Centre, York University, Toronto, Ontario M3J 1P3, Canada

**Abstract.** Assessing dependence within co-movements of financial instruments has been of much interest in risk management. Typically, indices of tail dependence are used to quantify the strength of such dependence, although many of the indices underestimate the strength. Hence, we advocate the use of a statistical procedure designed to estimate the maximal strength of dependence that can possibly occur among the co-movements. We illustrate the procedure using simulated and real data-sets.

*Key words and phrases:* extreme co-movement, maximal tail dependence, financial instrument, statistical hypothesis.

---

This research has been supported by the Natural Sciences and Engineering Research Council (NSERC) of Canada, and the national research organization Mathematics of Information Technology and Complex Systems (MITACS) of Canada.

\*Corresponding author; e-mail [Chen.Yang@mountsinai.org](mailto:Chen.Yang@mountsinai.org)

# 1 Introduction

The phenomenon of extreme co-movements manifests in a variety of problems (e.g., [Castillo et al., 2004](#), and references therein). In financial management, for example, this phenomenon arises when dealing with contagion ([Pericoli and Sbracia, 2011](#)), developing risk mitigation strategies such as portfolio diversification ([Durante et al., 2014](#)). These and many other applications have inspired prolific studies of how to assess dependence within extreme co-movements (e.g., [Bücher et al., 2015](#); [White et al., 2015](#), and references therein).

For this purpose, researchers have often employed tail dependence indices (e.g., [Castillo et al., 2004](#); [Frahm et al., 2005](#); [Cherubini et al., 2013](#), and references therein). Their definitions rely on the behaviour of the copula  $C : [0, 1]^2 \rightarrow [0, 1]$ , which arises from paired financial instruments, along the diagonal path  $(u, u)_{0 \leq u \leq 1}$  near the vertex  $\mathbf{0} := (0, 0)$  of the unit square. In particular, the parameter  $\kappa \in [1, \infty)$  in the equation

$$C(u, u) = \ell(u)u^\kappa, \tag{1.1}$$

where  $\ell$  is a slowly varying at 0 function, is called the lower tail order, which we henceforth call the tail order of *diagonal* dependence (TODD). The modifier *diagonal* has been added to emphasize the equality of the two copula arguments on the left-hand side of equation (1.1).

Interestingly, the asymptotic behaviour of  $C(u, u)$  may or may not reflect the *maximal* strength of tail dependence, as has been pointed out and illustrated by [Furman et al. \(2015, 2016\)](#). Hence, it becomes natural to seek a path, called a path of maximal tail dependence (MTD), along which the copula  $C$  behaves like  $\ell^*(u)u^{\kappa^*}$  for the smallest possible  $\kappa^*$  and some slowly varying at 0 function  $\ell^*$ . We note that this MTD path may not be unique, and may not coincide with the diagonal path  $(u, u)_{0 \leq u \leq 1}$ . Henceforth, we call  $\kappa^*$  the tail order of *maximal* dependence (TOMD), whose rigorous description will be given in the next section.

For the TOMD  $\kappa^*$ , basic statistical inference has been developed by [Sun et al. \(2020\)](#) for independent and identically distributed (iid) paired data. In practice, however, co-movements often arise from time-indexed stochastic processes, such as time series (e.g., [White et al., 2015](#), and references therein), whose generated data are inherently dependent. The iid-based results, therefore, need to be adjusted and extended. Fortunately, the block-structure of the estimator of [Sun et al. \(2020\)](#) facilitates the task, due to the fact that practically relevant time series give rise to nearly-independent data blocks when the gaps between the blocks are sufficiently wide. Nevertheless, serious work remains, and this is the main purpose of the present paper.

The rest is organized as follows. In [Section 2](#) we introduce TOMD and TODD estimators. In [Section 3](#) we discuss the estimators and prepare them for the analysis of real time series data.

In Section 4 we develop a dependent-data generating process and then illustrate and assess the estimators' performance. In Section 5 we explore the strength of extreme co-movements of a number of financial instruments, such as historical exchange rates of several currencies, stock market indices, and mixed financial instruments. Section 6 concludes the paper with a summary. To facilitate readability of the paper, a number of statistical tests, tables and graphs have been relegated to Appendix A, which consists of Sections A.1–A.3.

## 2 Tail-order estimators

For any bivariate copula  $C : [0, 1]^2 \rightarrow [0, 1]$ , a path of tail dependence (Furman et al., 2015) is defined as  $(\varphi(u), u^2/\varphi(u))_{0 \leq u \leq 1}$  for any function  $\varphi : [0, 1] \rightarrow [0, 1]$  that satisfies two admissibility conditions:

- (1)  $\varphi(u) \in [u^2, 1]$  for every  $u \in [0, 1]$ ,
- (2)  $\varphi(u) \rightarrow 0$  and  $u^2/\varphi(u) \rightarrow 0$  when  $u \downarrow 0$ .

Denote the set of all admissible functions by  $\mathcal{A}$ .

An admissible function  $\varphi^* \in \mathcal{A}$  that maximizes the functional  $\varphi \mapsto C(\varphi(u), u^2/\varphi(u))$  gives rise to a path  $(\varphi^*(u), u^2/\varphi^*(u))_{0 \leq u \leq 1}$  that we call a path of maximal tail dependence (MTD). There can be several maximizing functions  $\varphi^*$  and thus several MTD paths. For any of them, define  $\Pi^* : [0, 1] \rightarrow [0, 1]$  by

$$\Pi^*(u) = C(\varphi^*(u), u^2/\varphi^*(u)).$$

If there exists  $\kappa^*$  and a slowly varying at 0 function  $\ell^*$  such that

$$\Pi^*(u) = \ell^*(u)u^{\kappa^*}, \tag{2.1}$$

then  $\kappa^*$  is called the lower tail order of *maximal* dependence (TOMD). This  $\kappa^*$  is unique for the copula  $C$ , irrespective of the fact that there can be several admissible functions  $\varphi^*$  leading to it. As illustrated by Furman et al. (2015), the TOMD  $\kappa^*$  may or may not coincide with the TODD  $\kappa$ , with the Gaussian copula providing one of those rare examples when  $\kappa^* = \kappa$  (Furman et al., 2016).

Intuitively, the role of a maximal path, written generally as  $(\varphi^*(u), \psi^*(u))_{0 \leq u \leq 1}$ , is for each  $u \in (0, 1]$  to define the rectangle

$$\mathcal{R}_u(\mathbf{0}) := [0, \varphi^*(u)] \times [0, \psi^*(u)]$$

which

- (1) is a subset of the unit square  $[0, 1]^2$ ;
- (2) has the same area as  $[0, u]^2$ , and thus necessarily implies  $\psi^*(u) = u^2/\varphi^*(u)$ ;
- (3) when a large number of pairs are simulated from the copula  $C$ , the rectangle  $\mathcal{R}_u(\mathbf{0})$  contains at least as many simulated pairs as any other rectangle in the first quadrant of the plane with one of its vertices being  $\mathbf{0}$  and the area equal to  $u^2$ .

We now introduce an empirical estimator of the TOMD  $\kappa^*$ . Suppose that the underlying model is a bi-variate stationary time series  $(X_i, Y_i)$ ,  $i \in \mathbb{Z}$ , and let the pairs  $(X_1, Y_1), \dots, (X_n, Y_n)$  be observable. Hence, our data are  $(x_1, y_1), \dots, (x_n, y_n) \in \mathbb{R}^2$ . Next we separate the marginal distributions from the dependence structure, about which we learn from the bivariate pseudo-observations  $(u_1, v_1), \dots, (u_n, v_n) \in [0, 1]^2$ , which give rise to a scatterplot in the unit square  $[0, 1]^2$ , as well as to the empirical copula

$$C_n(u, v) := \frac{1}{n} \sum_{i=1}^n \mathbf{1}\{u_i \leq u, v_i \leq v\}, \quad u, v \in [0, 1].$$

In order to mitigate the potential influence of  $\ell^*$  (equation (2.1)) on the TOMD estimation, we focus on those observed pairs that fall into the rectangle

$$\mathcal{R}_{q,n}(\mathbf{0}) := [0, \varphi_n^*(q)] \times [0, q^2/\varphi_n^*(q)],$$

where

$$\varphi_n^*(q) = \arg \max_{x \in [q^2, 1]} C_n(x, q^2/x).$$

Various choices of  $q \in (0, 1]$  will be discussed later in this paper, for simulated and real data. We now only note that when  $q = 1$ , the rectangle is the unit square  $[0, 1]^2$ .

Hence, from all the pseudo observations  $(u_1, v_1), \dots, (u_n, v_n) \in [0, 1]^2$ , we single out those that are in  $\mathcal{R}_{q,n}(\mathbf{0})$ . We identify them by their indices, which we collect into the set

$$\mathcal{M}_{q,n} := \{i : (u_i, v_i) \in \mathcal{R}_{q,n}(\mathbf{0})\} \subseteq \{1, \dots, n\}.$$

Let  $m_{q,n} := \#(\mathcal{M}_{q,n})$  denote the cardinality of  $\mathcal{M}_{q,n}$ , that is, the number of the pairs  $(u_i, v_i)$  residing in  $\mathcal{R}_{q,n}(\mathbf{0})$ . Obviously,  $m_{q,n} \leq n$  and so when we make the assumption that  $m_{q,n}$  is sufficiently large, we also implicitly say that the underlying sample size  $n$  is large. The quantity

$$\Pi_n^*(q) := \frac{m_{q,n}}{n} = \frac{1}{n} \sum_{i=1}^n \mathbf{1}\{(u_i, v_i) \in \mathcal{R}_{q,n}(\mathbf{0})\}$$

is an empirical proxy for  $\Pi^*(q) = \mathbb{P}((U, V) \in \mathcal{R}_q(\mathbf{0}))$ .

**Note 2.1.** This paper is long, and we have tried – whenever reasonable – to avoid pedantic details of the proof. For example, results like  $\Pi_n^*(q)$  being a proxy for  $\Pi^*(q)$  would normally go without a proof, but to illustrate this instance, suppose that we wish to check the result. Since

$$\Pi_n^*(q) = \max_{x \in [q^2, 1]} C_n(x, q^2/x), \quad \Pi^*(q) = \max_{x \in [q^2, 1]} C(x, q^2/x)$$

for  $q \in (0, 1]$ , we have

$$\begin{aligned} |\Pi_n^*(q) - \Pi^*(q)| &\leq \max_{x \in [q^2, 1]} |C_n(x, q^2/x) - C(x, q^2/x)| \\ &\leq \sup_{u, v \in [0, 1]} |C_n(u, v) - C(u, v)| \xrightarrow{P} 0 \end{aligned}$$

when  $n \rightarrow \infty$ , where  $\xrightarrow{P}$  denotes convergence in probability. As we see from the classical results of [Kiefer and Wolfowitz \(1958\)](#), and [Kiefer \(1961\)](#), the convergence holds even almost surely. Much work has been done since these papers in order to relax the iid assumption, and we refer to, e.g., [Davydov and Zitikis \(2008\)](#), and [Kontorovich and Weiss \(2014\)](#) for results and references on the topic.

Next, we fix any  $m \geq 1$  such that  $m \leq m_{q,n}$ , which holds (Note [2.1](#)) with as large a probability as desired, assuming that  $n$  is sufficiently large. Then we assign the pairs  $(u_i, v_i)$ ,  $i \in \mathcal{M}_{q,n}$ , into  $\lceil m_{q,n}/m \rceil$  disjoint groups so that there can be at most one group with less than  $m$  pairs and all the other groups containing exactly  $m$  pairs. We collect the indices of the grouped pairs into the (disjoint) sets  $G_{j,q,n}$ ,  $1 \leq j \leq \lceil m_{q,n}/m \rceil$ , thus producing a partition of  $\mathcal{M}_{q,n}$ . We note that choosing an appropriate value of  $m$  is a delicate problem in practice, and we shall discuss it in great detail when working with simulated and real data later in this paper.

We define the *average block-minima estimator* of the TOMD  $\kappa^*$  as follows:

$$\hat{\kappa}_{m_{q,n}}^*(m, \theta, q) = \frac{1}{\lceil m_{q,n}/m \rceil} \sum_{j=1}^{\lceil m_{q,n}/m \rceil} \min_{i \in G_{j,q,n}} \frac{2T_\theta \circ F_{q, \mathcal{M}_{q,n}}(u_i, v_i)}{\log u_i + \log v_i - 2 \log q}, \quad (2.2)$$

where, for all  $u, v \in [0, 1]$ ,

$$F_{q, \mathcal{M}_{q,n}}(u, v) = \frac{1}{m_{q,n}} \sum_{i \in \mathcal{M}_{q,n}} \mathbb{1}\{u_i \leq u, v_i \leq v\}, \quad (2.3)$$

and, for all  $t \in (0, 1]$ ,

$$T_\theta(t) = \begin{cases} (t^\theta - 1)/\theta & \text{when } \theta > 0, \\ \log(t) & \text{when } \theta = 0. \end{cases}$$

For comparison, we also estimate the TODD  $\kappa$ . Its estimator is defined as follows (cf. [Gabaix and Ibragimov, 2011](#)). Denote

$$\mathcal{N}_{q,n} = \{i : (u_i, v_i) \in \mathcal{S}_q(\mathbf{0})\} \subseteq \{1, \dots, n\},$$

where  $\mathcal{S}_q(\mathbf{0}) = [0, q]^2$ . Let  $n_{q,n} := \#(\mathcal{N}_{q,n})$ , the cardinality of  $\mathcal{N}_{q,n}$ , that is,  $n_{q,n}$  is the number of pairs  $(u_i, v_i)$  in the square  $\mathcal{S}_q(\mathbf{0})$ . For each  $i = 1, \dots, n_{q,n}$ , denote  $w_i := q \min\{u_i^{-1}, v_i^{-1}\}$ . Furthermore, let  $w_{1:n_{q,n}} \geq \dots \geq w_{n_{q,n}:n_{q,n}}$  denote the ordered values of the  $w$ 's. Note that  $n_{q,n} = \max\{i : w_{i:n_{q,n}} \geq 1\}$ . We define the estimator of the TODD  $\kappa$  by

$$\hat{\kappa}_{n_{q,n}}^{\text{OLS}} = \frac{\sum_{i=1}^{n_{q,n}} (\log w_{i:n_{q,n}} - \overline{\log w}) \log(i - 0.5)}{\sum_{i=1}^{n_{q,n}} (\log w_{i:n_{q,n}} - \overline{\log w})^2}, \quad (2.4)$$

where  $\overline{\log w}$  denotes the average of all  $\log w_1, \dots, \log w_{n_{q,n}}$ . We refer to [Gabaix and Ibragimov \(2011\)](#) for an illuminating discussion of why 0.5 needs to be subtracted from  $i$  in  $\log(i - 0.5)$  when defining the estimator.

### 3 Justification of the estimators

In practice we cannot know whether slowly varying functions are present or not in equations (1.1) and (2.1). This poses a challenge. In this section, therefore, we adjust the methodology of [Sun et al. \(2020\)](#) so that we could tackle TOMD and TODD estimation under the uncertainty with respect to slowly varying functions. An important feature that will permeate our following considerations is a conditioning argument, whose main idea is based on the fact that extreme financial losses are those that are below a certain (small) threshold  $q \in (0, 1)$ , which are set by convention or regulation.

Hence, we are dealing with conditional copulas below  $q$ , which are ratios of probabilities. Via equation (2.1), we reduce these ratios to quantities like  $\ell^*(qu)/\ell^*(q)$ , which are close to 1 when  $q > 0$  is small, due to the very definition of slowly varying at 0 functions:

$$\frac{\ell^*(qu)}{\ell^*(q)} \rightarrow 1 \quad \text{when } q \downarrow 0, \quad (3.1)$$

and this limit holds irrespective of  $u > 0$ .

When choosing a small  $q > 0$  in practice, we should be mindful of the fact that the smaller the threshold  $q$ , the smaller the number  $m_{q,n}$  of pairs falling into the rectangle  $\mathcal{R}_{q,n}(\mathbf{0})$ . This obviously impedes statistical inference, and so we need to strike a balance between the values of  $q$  and  $m_{q,n}$ . We shall give a considerable thought to this issue when dealing with real data later in this paper.

### 3.1 Estimating the TOMD

We first recall a procedure for estimating the TOMD  $\kappa^*$  developed by [Sun et al. \(2020\)](#). By doing so, we also introduce the necessary notation for our following considerations. We start with equation (2.1) and express the conditional maximal tail probability as

$$\frac{\Pi^*(qu)}{\Pi^*(q)} = \frac{C(\varphi^*(qu), q^2 u^2 / \varphi^*(qu))}{C(\varphi^*(q), q^2 / \varphi^*(q))} = \frac{\ell^*(qu)(qu)^{\kappa^*}}{\ell^*(q)q^{\kappa^*}} \approx u^{\kappa^*} \quad (3.2)$$

when  $0 < q \approx 0$ , due to statement (3.1). Hence, we have the approximate bound

$$\frac{C(\varphi(qu), q^2 u^2 / \varphi(qu))}{C(\varphi^*(q), q^2 / \varphi^*(q))} \lesssim u^{\kappa^*} \quad (3.3)$$

that holds for every  $\varphi \in \mathcal{A}$ . With the notations  $\tilde{u} = \varphi(qu) / \varphi^*(q)$  and  $\tilde{v} = u^2 \varphi^*(q) / \varphi(qu)$ , we turn approximate bound (3.3) into

$$\frac{C(\varphi^*(q)\tilde{u}, q^2 \tilde{v} / \varphi^*(q))}{C(\varphi^*(q), q^2 / \varphi^*(q))} \lesssim u^{\kappa^*}.$$

Since  $u^{\kappa^*} = (\tilde{u}\tilde{v})^{\kappa^*/2}$ , this leads to

$$\kappa^* \lesssim \frac{2 \log F_q^*(\tilde{u}, \tilde{v})}{\log \tilde{u} + \log \tilde{v}}, \quad (3.4)$$

where  $F_q^* : [0, 1]^2 \rightarrow [0, 1]$  is defined by

$$F_q^*(u, v) = \frac{C(u\varphi^*(q), vq^2 / \varphi^*(q))}{C(\varphi^*(q), q^2 / \varphi^*(q))}. \quad (3.5)$$

This gives a theoretical basis for building an empirical estimator of the TOMD  $\kappa^*$ .

Namely, given pseudo observations  $(u_1, v_1), \dots, (u_n, v_n) \in [0, 1]^2$ , and also a small and fixed  $q > 0$ , the TOMD  $\kappa^*$  is estimated using the following four-step procedure:

- (1) using all the pairs available in the unit square  $[0, 1]^2$ , compute an empirical estimate of  $\varphi^*(q)$  by maximizing  $C_n(x, q^2/x)$  with respect to  $x \in [q^2, 1]$ ;
- (2) extract the set  $\mathcal{P}_{q,n}$  of those pairs  $(u_k, v_k)$  that are in the rectangle  $\mathcal{R}_{q,n}(\mathbf{0})$ , then collect the indices of the pairs into the set  $\mathcal{M}_{q,n}$ , and denote the cardinality of  $\mathcal{M}_{q,n}$  by  $m_{q,n}$ ;
- (3) randomly assign the pairs of  $\mathcal{P}_{q,n}$  into  $\lceil m_{q,n}/m \rceil$  disjoint groups of pairs, whose indices partition  $\mathcal{M}_{q,n}$  into groups  $G_{1,q,n}, \dots, G_{\lceil m_{q,n}/m \rceil, q,n}$  with at most one of them having fewer than  $m$  elements, while all the other groups having exactly  $m$  elements;
- (4) compute the average block-minima estimator of the TOMD  $\kappa^*$  using formula (2.2).

To appreciate formula (2.2) in view of the above procedure, note that when  $i \in \mathcal{M}_{q,n}$  we have

$$F_{q,\mathcal{M}_{q,n}}(u_i, v_i) = \frac{1}{m_{q,n}} \# \{k \in \mathcal{M}_{q,n} : u_k \leq u_i, v_k \leq v_i\} = F_{q,\mathcal{M}_{q,n}}^*(\tilde{u}_i, \tilde{v}_i),$$

where  $\tilde{u}_i = u_i/\varphi_n^*(q)$ ,  $\tilde{v}_i = v_i\varphi_n^*(q)/q^2$ , and

$$F_{q,\mathcal{M}_{q,n}}^*(u, v) := \frac{1}{m_{q,n}} \sum_{k \in \mathcal{M}_{q,n}} \mathbb{1}\{\tilde{u}_k \leq u, \tilde{v}_k \leq v\}. \quad (3.6)$$

Hence, estimator (2.2) can be rewritten as

$$\hat{\kappa}_{m_{q,n}}^*(m, \theta, q) = \frac{1}{\lceil m_{q,n}/m \rceil} \sum_{j=1}^{\lceil m_{q,n}/m \rceil} \min_{i \in G_{j,q,n}} \frac{2T_\theta \circ F_{q,\mathcal{M}_{q,n}}^*(\tilde{u}_i, \tilde{v}_i)}{\log \tilde{u}_i + \log \tilde{v}_i}. \quad (3.7)$$

### 3.2 Estimating the TODD

For comparison, we estimate the TODD  $\kappa$ . With some modifications, we follow the spirit of Section 3.1. Namely, in view of equation (1.1), we have

$$\frac{C(qu, qu)}{C(q, q)} = \frac{\ell(qu)(qu)^\kappa}{\ell(q)q^\kappa} \approx u^\kappa \quad (3.8)$$

when  $0 < q \approx 0$ , due to statement (3.1). To see an analogy between equations (3.8) and (3.2), set  $\varphi^*(u) = u$  in statement (3.2). Next, we rewrite approximate equation (3.8) as

$$\mathbb{P}(\max\{U, V\} \leq qu \mid \max\{U, V\} \leq q) \approx u^\kappa. \quad (3.9)$$

With the notation  $z := u^{-1}$ , equation (3.9) turns into

$$\mathbb{P}(W \geq z \mid W \geq 1) \approx z^{-\kappa}, \quad (3.10)$$

where  $W = q \min\{U^{-1}, V^{-1}\}$ .

To implement approximate equation (3.10) on data, we need its empirical version. For this, modulus some adjustments, we follow the ideas of Gabaix and Ibragimov (2011). In terms of the order statistics (e.g., David and Nagaraja, 2003; Arnold et al., 2008; Ahsanullah et al., 2013)  $w_{1:n_{q,n}} \geq \dots \geq w_{n_{q,n}:n_{q,n}}$ , the empirical version of statement (3.10) becomes

$$i/n_{q,n} \approx w_{i:n_{q,n}}^{-\kappa}, \quad i = 1, \dots, n_{q,n}. \quad (3.11)$$

Taking logarithms of both sides of approximate equation (3.11), we obtain

$$\log i \approx \log n_{q,n} - \kappa \log w_{i:n_{q,n}}.$$

We now arrive at an estimator of  $\kappa$  as the slope of the least squares regression line fitted to the scatterplot of the pairs  $(\log(i - 0.5), \log w_{i:n_{q,n}})$ ,  $i = 1, \dots, n_{q,n}$ . This gives estimator (2.4).



### 3.3 Estimator's performance justification

We use all  $n$  available pseudo observations  $(u_i, v_i)$  to get estimates of  $C$ ,  $\varphi^*(q)$ ,  $\mathcal{R}_q(\mathbf{0})$ , and  $\Pi^*(q)$ . Since in our applications the sample size  $n$  is large, it is reasonable to assume that the estimates are close – or as close as we can possibly get them – to their population versions, and we thus adopt the same notations for them, that is, we skip the subscript  $n$ .

The number  $m_q$  of the observed pairs in the estimated rectangle is relatively small, and thus their variability matters. We thus face the question of whether or not  $m_q$  is sufficiently large in order to make reliable statistical decisions. To answer this question, we theoretically explore the convergence of the simplified estimator

$$\hat{\kappa}_{m_q}^*(m, 0, q) = \frac{1}{\lceil m_q/m \rceil} \sum_{j=1}^{\lceil m_q/m \rceil} \min_{i \in G_{j,q}} \frac{2T_0(C(U_{i,q}, V_{i,q})/\Pi^*(q))}{\log U_{i,q} + \log V_{i,q} - 2 \log q} \quad (3.12)$$

when  $m_q \rightarrow \infty$ , where  $(U_{i,q}, V_{i,q})$ ,  $i \in \mathcal{M}_q$ , are random iid pairs, each following the conditional cdf  $F_q : [0, 1]^2 \rightarrow [0, 1]$  defined by

$$\begin{aligned} F_q(u, v) &:= \mathbb{P}(U \leq u, V \leq v \mid (U, V) \in \mathcal{R}_q(\mathbf{0})) \\ &= \frac{1}{\Pi^*(q)} C(\min\{u, \varphi^*(q)\}, \min\{v, q^2/\varphi^*(q)\}). \end{aligned}$$

Thus,  $F_q(u, v) = C(u, v)/\Pi^*(q)$  for all  $(u, v) \in \mathcal{R}_q(\mathbf{0})$ . By the law of large numbers, when  $m_q \rightarrow \infty$ , we have

$$\hat{\kappa}_{m_q}^*(m, 0, q) \xrightarrow{\mathbb{P}} \kappa^*(m, 0, q) := \mathbb{E} \left[ \min_{i \in G_{1,q}} \frac{2T_0(C(U_{i,q}, V_{i,q})/\Pi^*(q))}{\log U_{i,q} + \log V_{i,q} - 2 \log q} \right]. \quad (3.13)$$

At first sight, assuming independence of the pairs  $(U_{i,q}, V_{i,q})$ ,  $i \in \mathcal{M}_q$ , might be alarming, given that we aim at analyzing (dependent) time series data. However, since for reasons of mitigating the influence of slowly varying function on the estimator, we shall use only those observed pairs that are in a (small) neighbourhood of  $\mathbf{0}$ . This gives rise to nearly independent data, as we shall see in Section A.1. There is, of course, a gap between independent variables and nearly independent (e.g., white noise) ones, but our estimator, with its block structure, is fairly robust with respect to dependence (Section 4). Hence, we can comfortably assume that the random pairs  $(U_{i,q}, V_{i,q})$ ,  $i \in \mathcal{M}_q$ , are iid.

The following theorem shows that by choosing  $m \geq 1$  and  $q > 0$  appropriately, we can make  $\kappa^*(m, 0, q)$  as close to the TOMD  $\kappa^*$  as desired, and thus by statement (3.13), the estimator  $\hat{\kappa}_{m_q}^*(m, 0, q)$  gets close to the TOMD  $\kappa^*$ .

**Theorem 3.1.** *Let  $q \in (0, 1]$  be any, and let the cdf  $F_q^*$  be PQD, that is,  $F_q^*(u, v) \geq uv$  for all  $u, v \in [0, 1]$ . Furthermore, let the functions  $\varphi^*(u)$  and  $\psi^*(u) := u^2/\varphi^*(u)$  be strictly increasing. Then  $\kappa^*(m, 0, q)$  can be made as close to  $\kappa^*$  as desired by taking sufficiently large  $m \geq 1$  and sufficiently small  $q > 0$ .*

*Proof.* The proof is long, but we believe that it is necessary to present it in order to show why and how the estimator works. We start by expressing  $\kappa^*(m, 0, q)$  in terms of the survival function of the random variable

$$\xi_q := \frac{2 \log(C(U_q, V_q)/\Pi^*(q))}{\log(U_q V_q/q^2)}. \quad (3.14)$$

That is,  $\kappa^*(m, 0, q)$  is equal to the integral  $\int_0^\infty \mathbb{P}(\xi_q > x)^m dx$ , because the cardinality of the set  $G_{1,q}$  is  $m$  and the pairs  $(U_{i,q}, V_{i,q})$ ,  $i \in G_{1,q}$ , are iid. With the notation

$$(\tilde{U}_q, \tilde{V}_q) := \left( \frac{U_q}{\varphi^*(q)}, \frac{V_q \varphi^*(q)}{q^2} \right),$$

we rewrite  $\xi_q$  as

$$\xi_q = \frac{2 \log(C(U_q, V_q)/\Pi^*(q))}{\log(U_q/\varphi^*(q)) + \log(V_q \varphi^*(q)/q^2)} = \frac{2 \log F_q^*(\tilde{U}_q, \tilde{V}_q)}{\log \tilde{U}_q + \log \tilde{V}_q} \in [0, 2], \quad (3.15)$$

where the inclusion into the interval  $[0, 2]$  is due to the assumed PQD property of  $F_q^*$ . Hence,

$$\kappa^*(m, 0, q) = \int_0^2 \mathbb{P}(\xi_q > x)^m dx. \quad (3.16)$$

**Note 3.1.** The meaning of equations (3.15) is to scale the pair  $(U_q, V_q) \in \mathcal{R}_q(\mathbf{0})$  into  $(\tilde{U}_q, \tilde{V}_q) \in [0, 1]^2$ . This allows to shift our focus from the behaviour of random pairs with respect to  $q \downarrow 0$  toward the behaviour of  $F_q^*$  and the scaling parameters  $\varphi^*(q)$  and  $q^2/\varphi^*(q)$ .

Since  $(U_q, V_q) \in \mathcal{R}_q(\mathbf{0})$  and the functions  $\varphi^*$  and  $z \mapsto z^2/\varphi^*(z)$  are increasing, we have

$$(\tilde{U}_q^*, \tilde{V}_q^*) := \left( \frac{\varphi^*(\sqrt{U_q V_q})}{\varphi^*(q)}, \frac{(\sqrt{U_q V_q})^2/\varphi^*(\sqrt{U_q V_q})}{q^2/\varphi^*(q)} \right) \in [0, 1]^2.$$

Hence,

$$\begin{aligned} F_q^*(\tilde{U}_q^*, \tilde{V}_q^*) &= \frac{1}{\Pi^*(q)} C(\varphi^*(\sqrt{U_q V_q}), U_q V_q / \varphi^*(\sqrt{U_q V_q})) \\ &= \frac{1}{\Pi^*(q)} \sup_{x \in [U_q V_q, 1]} C(x, U_q V_q / x) \\ &\geq \frac{1}{\Pi^*(q)} C(U_q, V_q) \\ &= F_q^*(\tilde{U}_q, \tilde{V}_q). \end{aligned}$$

Since  $\tilde{U}_q^* \tilde{V}_q^* = \tilde{U}_q \tilde{V}_q = U_q V_q / q^2 \in (0, 1)$ , we therefore arrive at the bound

$$\frac{2 \log F_q^*(\tilde{U}_q^*, \tilde{V}_q^*)}{\log \tilde{U}_q^* + \log \tilde{V}_q^*} \leq \frac{2 \log F_q^*(\tilde{U}_q, \tilde{V}_q)}{\log \tilde{U}_q + \log \tilde{V}_q}. \quad (3.17)$$

Note that

$$\begin{aligned} \frac{2 \log F_q^*(\tilde{U}_q^*, \tilde{V}_q^*)}{\log \tilde{U}_q^* + \log \tilde{V}_q^*} &= \frac{2 \log \left( C(\varphi^*(\sqrt{U_q V_q}), (\sqrt{U_q V_q})^2 / \varphi^*(\sqrt{U_q V_q})) / \Pi^*(q) \right)}{\log(U_q V_q / q^2)} \\ &= \frac{2 \log (\Pi^*(\sqrt{U_q V_q}) / \Pi^*(q))}{\log(U_q V_q / q^2)}. \end{aligned} \quad (3.18)$$

Due to equation (2.1), we have

$$\frac{\Pi^*(\sqrt{U_q V_q})}{\Pi^*(q)} = \frac{\ell^*(\sqrt{U_q V_q})}{\ell^*(q)} \left( \frac{U_q V_q}{q^2} \right)^{\kappa^*/2}$$

and thus, continuing with equations (3.18) and taking into account bound (3.17), we obtain

$$\frac{2 \log F_q^*(\tilde{U}_q, \tilde{V}_q)}{\log \tilde{U}_q + \log \tilde{V}_q} \geq \frac{2 \log(\ell^*(\sqrt{U_q V_q}) / \ell^*(q))}{\log(U_q V_q / q^2)} + \kappa^*. \quad (3.19)$$

With the notation

$$o_q := \frac{2 \log(\ell^*(\sqrt{U_q V_q}) / \ell^*(q))}{\log(U_q V_q / q^2)},$$

bound (3.19) takes the form

$$\xi_q \geq \max\{0, o_q + \kappa^*\}. \quad (3.20)$$

We next prove  $o_q \xrightarrow{\mathbb{P}} 0$  when  $q \downarrow 0$ .

With the notation  $W_q = \sqrt{U_q V_q} / q$ , the statement is equivalent to

$$o_q = \frac{\log(\ell^*(q W_q) / \ell^*(q))}{\log W_q} \xrightarrow{\mathbb{P}} 0. \quad (3.21)$$

Hence, we first fix any  $\epsilon > 0$ . Then we take any  $\delta > 0$  and partition the sample space into three events:  $\{W_q < \delta\}$ ,  $\{\delta \leq W_q \leq 1 - \delta\}$  and  $\{W_q > 1 - \delta\}$ . We have the bound

$$\begin{aligned} &\mathbb{P} \left( \left| \frac{\log(\ell^*(q W_q) / \ell^*(q))}{\log W_q} \right| > \epsilon \right) \\ &\leq \mathbb{P} \left( \sup_{w \in [\delta, 1-\delta]} \left| \frac{\log(\ell^*(q w) / \ell^*(q))}{\log w} \right| > \epsilon \right) + \mathbb{P}(W_q < \delta) + \mathbb{P}(W_q > 1 - \delta). \end{aligned} \quad (3.22)$$

Since  $\ell^*$  is slowly varying at 0, we have  $\ell^*(q w) / \ell^*(q) \rightarrow 1$  when  $q \downarrow 0$  for every  $w \in (0, 1]$ . The convergence is even uniform in  $w \in [\delta, 1]$  for any fixed  $\delta > 0$ , which implies (Bojanic and

Seneta, 1971, Lemma 1, p. 310) that  $\sup_{w \in [\delta, 1]} |\log(\ell^*(qw)/\ell^*(q))|$  converges to 0 when  $q \downarrow 0$ . Hence, we conclude from bound (3.22) that, for any  $\epsilon > 0$  and  $\delta > 0$ ,

$$\limsup_{q \rightarrow 0} \mathbb{P} \left( \left| \frac{\log(\ell^*(qW_q)/\ell^*(q))}{\log W_q} \right| > \epsilon \right) \leq \limsup_{q \rightarrow 0} \mathbb{P}(W_q < \delta) + \limsup_{q \rightarrow 0} \mathbb{P}(W_q > 1 - \delta). \quad (3.23)$$

Note that the left-hand side of bound (3.23) does not depend on  $\delta > 0$ . As to the first probability on the right-hand side of bound (3.23), we have the following result:

$$\begin{aligned} \mathbb{P}(W_q \leq \delta) &= \mathbb{P}(U_q V_q \leq \delta \varphi^*(q) \delta q^2 / \varphi^*(q)) \\ &\leq \mathbb{P}(U_q \leq \delta \varphi^*(q)) + \mathbb{P}(V_q \leq \delta q^2 / \varphi^*(q)) \\ &= \frac{1}{\Pi^*(q)} (C(\delta \varphi^*(q), q^2 / \varphi^*(q)) + C(\varphi^*(q), \delta q^2 / \varphi^*(q))) \\ &\leq \frac{2\Pi^*(q\sqrt{\delta})}{\Pi^*(q)} \rightarrow 2\delta^{\kappa^*/2} \end{aligned} \quad (3.24)$$

when  $q \downarrow 0$ , where we have used equation (2.1) and property (3.1).

We tackle the second probability on the right-hand side of bound (3.23) in a different way, starting as follows:

$$\mathbb{P}(W_q > 1 - \delta) = \mathbb{P}(\tilde{U}_q \tilde{V}_q > (1 - \delta)^2) \leq \mathbb{P}(F_q^*(\tilde{U}_q, \tilde{V}_q) > (1 - \delta)^2), \quad (3.25)$$

where the bound holds because  $F_q^*$  is PQD, that is,  $F_q^*(u, v) \geq uv$  for all  $u, v \in [0, 1]$ . With

$$K_q^*(t) := \mathbb{P}(F_q^*(\tilde{U}_q, \tilde{V}_q) \leq t)$$

we continue bound (3.25) and have

$$\mathbb{P}(W_q > 1 - \delta) = 1 - K_q^*((1 - \delta)^2) \leq 1 - (1 - \delta)^2 \quad (3.26)$$

for every  $q \in (0, 1]$  because

$$K_q^*(t) \geq \mathbb{P}(F_q^*(\tilde{U}_q, 1) \leq t) = \mathbb{P}(G_q(\tilde{U}_q) \leq t) = \mathbb{P}(\tilde{U}_q \leq G_q^{-1}(t)) = G_q \circ G_q^{-1}(t) = t,$$

where  $G_q : [0, 1] \rightarrow [0, 1]$  denotes the cdf of  $\tilde{U}_q$  given by

$$G_q(u) = \frac{C(\varphi^*(q)u, q^2/\varphi^*(q))}{C(\varphi^*(q), q^2/\varphi^*(q))} = \frac{C(\varphi^*(q)u, q^2/\varphi^*(q))}{\Pi^*(q)}.$$

Hence, in view of bounds (3.24) and (3.26), the entire right-hand side of bound (3.23) vanishes when  $\delta \downarrow 0$ . This concludes the proof of statement (3.21).

Fix any  $\epsilon \in (0, \kappa^*)$ . From equation (3.16), we have the upper bound

$$\kappa^*(m, 0, q) \leq \kappa^* + \epsilon + \int_{\kappa^* + \epsilon}^2 \mathbb{P}(\xi_q > x)^m dx. \quad (3.27)$$

For the lower bound, we start as follows:

$$\begin{aligned}\kappa^*(m, 0, q) &= \kappa^* - \epsilon - \int_0^{\kappa^* - \epsilon} 1 - \mathbb{P}(\xi_q > x)^m dx + \int_{\kappa^* + \epsilon}^2 \mathbb{P}(\xi_q > x)^m dx \\ &\geq \kappa^* - \epsilon - (\kappa^* - \epsilon)m\mathbb{P}(\xi_q \leq \kappa^* - \epsilon) + \int_{\kappa^* + \epsilon}^2 \mathbb{P}(\xi_q > x)^m dx.\end{aligned}\quad (3.28)$$

Using bound (3.20), we obtain

$$\begin{aligned}\mathbb{P}(\xi_q \leq \kappa^* - \epsilon) &\leq \mathbb{P}(\max\{0, o_q + \kappa^*\} \leq \kappa^* - \epsilon) \\ &= \mathbb{P}(o_q \leq -\epsilon, o_q + \kappa^* > 0) + \mathbb{P}(o_q + \kappa^* \leq 0) \\ &= 2\mathbb{P}(|o_q| \geq \epsilon),\end{aligned}\quad (3.29)$$

which can be made as small as desired by choosing a small  $q > 0$ . Hence, due to bounds (3.27)–(3.29), for any  $m \geq 1$  we can choose sufficiently small  $\epsilon > 0$  and  $q > 0$  such that  $\kappa^*(m, 0, q)$  becomes as close to  $\kappa^*$  as desired, provided that the integral  $\int_{\kappa^*}^2 \mathbb{P}(\xi_q > x)^m dx$  can be made as small as needed by choosing a sufficiently large  $m$ . We prove the latter fact next, without loss of generality assuming that  $\kappa^* < 2$ , which prevents  $F_q^*$  from being the independence copula.

By the Lebesgue dominated convergence theorem, the integral  $\int_{\kappa^*}^2 \mathbb{P}(\xi_q > x)^m dx$  converges to 0 when  $m \rightarrow \infty$  provided that  $\mathbb{P}(\xi_q > x) < 1$  for all  $x \in (\kappa^*, 2)$ . Hence, we need to show that

$$\mathbb{P}(\xi_q \leq \kappa^* + h) > 0 \quad \text{for every } h \in (0, 2 - \kappa^*). \quad (3.30)$$

The proof follows the idea of Sun et al. (2020, Theorem 3.2), but there are substantial adjustments, which we present next.

We start with the bound

$$\mathbb{P}(\xi_q \leq \kappa^* + h) = \mathbb{P}\left(\frac{2 \log F_q^*(\tilde{U}_q, \tilde{V}_q)}{\log \tilde{U}_q + \log \tilde{V}_q} \leq \frac{2 \log w_0^{\kappa^* + h}}{\log w_0^2}\right) \geq \mathbb{P}\left((\tilde{U}_q, \tilde{V}_q) \in B_{q,h}\right), \quad (3.31)$$

where (see Figure 3.1)

$$B_{q,h} := \{(u, v) \in [0, 1]^2 : uv \leq w_0^2, F_q^*(u, v) > w_0^{\kappa^* + h}\}$$

for some  $w_0 \in (0, 1)$ . With the notation  $w_0 = \sqrt{u_q v_q}$ , we have

$$u_q = \varphi^*(qw_0)/\varphi^*(q), \quad v_q = w_0^2 \varphi^*(q)/\varphi^*(qw_0),$$

and

$$F_q^*(u_q, v_q) = \frac{\ell^*(qw_0)}{\ell^*(q)} w_0^{\kappa^*} \approx w_0^{\kappa^*} > w_0^{\kappa^* + h}.$$

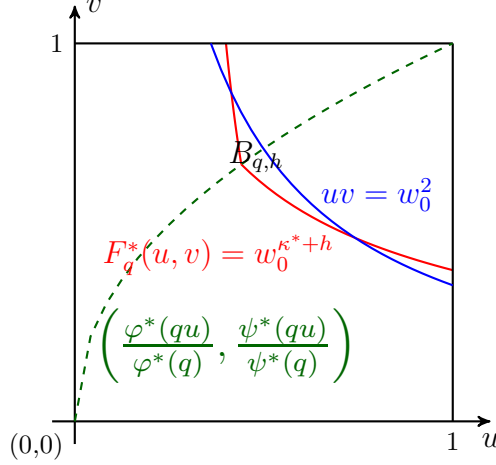


Figure 3.1: The area  $B_{q,h}$  and associated curves.

Hence,  $F_q^*(u_q, v_q) > w_0^{\kappa^*+h}$  for sufficiently small  $q > 0$  (depending on  $w_0$  and  $h$ ). Note that

$$F_q^*\left(\frac{\varphi^*(qw_0^{1+h/2\kappa^*})}{\varphi^*(q)}, \frac{w_0^{2+h/\kappa^*}\varphi^*(q)}{\varphi^*(qw_0^{1+h/2\kappa^*})}\right) = \frac{\Pi^*(qw_0^{1+h/2\kappa^*})}{\Pi^*(q)} \approx w_0^{\kappa^*+h/2}.$$

We have

$$F_q^*\left(\frac{\varphi^*(qw_0^{1+h/2\kappa^*})}{\varphi^*(q)}, \frac{w_0^{2+h/\kappa^*}\varphi^*(q)}{\varphi^*(qw_0^{1+h/2\kappa^*})}\right) > w_0^{\kappa^*+h}$$

for sufficiently small  $q > 0$  (depending on  $w_0$  and  $h$ ). By denoting

$$u_{q,h} = \frac{\varphi^*(qw_0^{1+h/2\kappa^*})}{\varphi^*(q)}, \quad v_{q,h} = \frac{w_0^{2+h/\kappa^*}\varphi^*(q)}{\varphi^*(qw_0^{1+h/2\kappa^*})},$$

we have  $u_{q,h}v_{q,h} = w_0^{2+h/\kappa^*} < w_0^2$ . Thus,  $(u_{q,h}, v_{q,h}) \in B_{q,h}$ . In particular,  $(u_{q,0}, v_{q,0}) = (u_q, v_q)$ . Since  $\varphi^*$  and  $\psi^*$  are strictly increasing functions, we have  $u_{q,h} < u_q$  and  $v_{q,h} < v_q$ , and so the rectangle (see Figure 3.2)

$$E_{q,h} := (u_{q,h}, u_q] \times (v_{q,h}, v_q]$$

is a non-empty subset of  $B_{q,h}$ . We have

$$\begin{aligned} \mathbb{P}((\tilde{U}_q, \tilde{V}_q) \in E_{q,h}) &= F_q^*(u_q, v_q) - F_q^*(u_q, v_{q,h}) - F_q^*(u_{q,h}, v_q) + F_q^*(u_{q,h}, v_{q,h}) \\ &= \frac{1}{\Pi^*(q)} \left[ C(\varphi^*(qw_0), \psi^*(qw_0)) - C(\varphi^*(qw_0), \psi^*(qw_0^{1+h/2\kappa^*})) \right. \\ &\quad \left. - C(\varphi^*(qw_0^{1+h/2\kappa^*}), \psi^*(qw_0)) + C(\varphi^*(qw_0^{1+h/2\kappa^*}), \psi^*(qw_0^{1+h/2\kappa^*})) \right] \\ &\geq \frac{w_0^{\kappa^*}}{\ell^*(q)} \left[ \ell^*(qw_0) - 2\ell^*(qw_0^{1+h/4\kappa^*})w_0^{h/4} + \ell^*(qw_0^{1+h/2\kappa^*})w_0^{h/2} \right] \\ &\rightarrow w_0^{\kappa^*}(1 - w_0^{h/4})^2 > 0 \end{aligned}$$

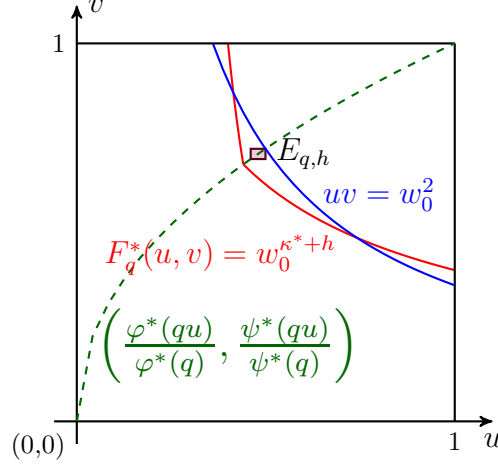


Figure 3.2: The rectangle  $E_{q,h} \subset B_{q,h}$  and associated curves.

when  $q \downarrow 0$ . In summary,  $\mathbb{P}((\tilde{U}_q, \tilde{V}_q) \in E_{q,h}) > 0$  for sufficiently small  $q > 0$  (depending on  $w_0$  and  $h$ ). This completes the proof of Theorem 3.1.  $\square$

### 3.4 Examples of, and insights into, $F_q^*$

In addition to  $F_q^*$ ,  $q \in (0, 1]$ , we next also discuss the limit

$$F_0^*(u, v) := \lim_{q \downarrow 0} F_q^*(u, v), \quad u, v \in [0, 1].$$

**Example 3.1.** The Marshall-Olkin (M-O) copula  $C_{a,b} : [0, 1]^2 \rightarrow [0, 1]$  is defined by

$$C_{a,b}(u, v) = \min(u^{1-a}v, uv^{1-b})$$

with parameters  $a, b \in [0, 1]$ . For every  $q \in [0, 1]$ , we have (Furman et al., 2015)  $\varphi^*(q) = q^{2b/(a+b)}$  and  $\psi^*(q) = q^{2a/(a+b)}$ , and so  $\Pi^*(u) = u^{\kappa^*}$  with the TOMD  $\kappa^* = 2 - 2ab/(a+b)$ .

Consequently, in view of definition (3.5), we have

$$\begin{aligned} F_q^*(u, v) &= \frac{\min\{(q^{2b/(a+b)}u)^{1-a}(q^{2a/(a+b)}v), (q^{2b/(a+b)}u)(q^{2a/(a+b)}v)^{1-b}\}}{q^{2-2ab/(a+b)}} \\ &= \min\{u^{1-a}v, uv^{1-b}\}, \end{aligned}$$

which is equal to  $C_{a,b}(u, v)$ . Hence,  $F_0^* = C_{a,b}$ . This implies that both  $F_q^*$  and  $F_0^*$  are PQD, because  $C_{a,b}$  is such.

**Example 3.2.** The generalized Clayton (GC) copula  $C_{\gamma_0, \gamma_1} : [0, 1]^2 \rightarrow [0, 1]$  is defined by

$$C_{\gamma_0, \gamma_1}(u, v) = u^{\gamma_1/\gamma^*} (u^{-1/\gamma^*} + v^{-1/\gamma_0} - 1)^{-\gamma_0} \quad (3.32)$$

with parameters  $\gamma_0 > 0$  and  $\gamma_1 \geq 0$ , and the notation  $\gamma^* := \gamma_0 + \gamma_1$ . Hence, we have

$$\begin{aligned} F_q^*(u, v) &= u^{\gamma_1/\gamma^*} \left( \frac{(\varphi^*(q)u)^{-1/\gamma^*} + (\psi^*(q)v)^{-1/\gamma_0} - 1}{\varphi^*(q)^{-1/\gamma^*} + \psi^*(q)^{-1/\gamma_0} - 1} \right)^{-\gamma_0} \\ &= u \left( \frac{\varphi^*(q)^{-1/\gamma^*} + (\psi^*(q)v)^{-1/\gamma_0} u^{1/\gamma^*} - u^{1/\gamma^*}}{\varphi^*(q)^{-1/\gamma^*} + \psi^*(q)^{-1/\gamma_0} - 1} \right)^{-\gamma_0} \\ &\geq u \left( \frac{\varphi^*(q)^{-1/\gamma^*} + (\psi^*(q)v)^{-1/\gamma_0} - 1}{\varphi^*(q)^{-1/\gamma^*} + \psi^*(q)^{-1/\gamma_0} - 1} \right)^{-\gamma_0} \\ &\geq u \left( \frac{(\psi^*(q)v)^{-1/\gamma_0}}{\psi^*(q)^{-1/\gamma_0}} \right)^{-\gamma_0} = uv. \end{aligned}$$

This shows that  $F_q^*$  is PQD.

Note that  $\varphi^*(q)$  satisfies (Furman et al., 2015, Eq. (6.1))

$$\varphi^*(q)^{-1/\gamma_0}(\varphi^*(q)^{-1/\gamma^*} - (\gamma_1/\gamma^*)) = (1 - (\gamma_1/\gamma^*))q^{-2/\gamma_0},$$

which reduces to  $\varphi^*(q)^{-1/\gamma^*} - (\gamma_1/\gamma^*) = (1 - (\gamma_1/\gamma^*))\psi^*(q)^{-1/\gamma_0}$  and gives

$$\begin{aligned} F_q^*(u, v) &= u^{\gamma_1/\gamma^*} \left( \frac{((1 - (\gamma_1/\gamma^*))\psi^*(q)^{-1/\gamma_0} + (\gamma_1/\gamma^*))u^{-1/\gamma^*} + (\psi^*(q)v)^{-1/\gamma_0} - 1}{(2 - (\gamma_1/\gamma^*))\psi^*(q)^{-1/\gamma_0} - (\gamma_0/\gamma^*)} \right)^{-\gamma_0} \\ &\rightarrow u^{\gamma_1/\gamma^*} \left( \frac{[1 - (\gamma_1/\gamma^*)]u^{-1/\gamma^*} + v^{-1/\gamma_0}}{2 - (\gamma_1/\gamma^*)} \right)^{-\gamma_0} =: F_0^*(u, v) \end{aligned}$$

when  $q \downarrow 0$ .

We next relate  $F_0^*$  and the TOMD  $\kappa^*$  via the bound

$$F_0^*(u, v) \leq (uv)^{\kappa^*/2} \quad (3.33)$$

for all  $u, v \in [0, 1]$ , where (Furman et al., 2015)

$$\kappa^* = 1 + \frac{\gamma_1}{\gamma_1 + 2\gamma_0}. \quad (3.34)$$

For any  $q \in (0, 1)$ , maximizing  $F_0^*(x, q^2/x)$  over  $x \in [q^2, 1]$  is equivalent to maximizing

$$x \mapsto \frac{\gamma_1}{\gamma^*} \log x - \gamma_0 \log \left( \frac{[1 - (\gamma_1/\gamma^*)]x^{-1/\gamma^*} + (q^2/x)^{-1/\gamma_0}}{2 - (\gamma_1/\gamma^*)} \right).$$

The first-order condition is

$$\frac{\gamma_1}{\gamma^* x} - \frac{\gamma_0[1 - (\gamma_1/\gamma^*)](-1/\gamma^*)x^{-1/\gamma^*-1} + q^{-2/\gamma_0}x^{1/\gamma_0-1}}{[1 - (\gamma_1/\gamma^*)]x^{-1/\gamma^*} + (q^2/x)^{-1/\gamma_0}} = 0,$$

which reduces to  $x^{-1/\gamma^*} = (q^2/x)^{-1/\gamma_0}$  and gives the solution  $x^* = q^{2\gamma^*/(\gamma^*+\gamma_0)}$ . Consequently,

$$\begin{aligned} \max_{x \in [q^2, 1]} F_0^*(x, q^2/x) &= F_0^*(q^{2\gamma^*/(\gamma^*+\gamma_0)}, q^{2\gamma_0/(\gamma^*+\gamma_0)}) \\ &= q^{2\gamma_1/(\gamma^*+\gamma_0)} q^{2\gamma_0/(\gamma^*+\gamma_0)} \\ &= q^{1+\gamma_1/(\gamma_1+2\gamma_0)}. \end{aligned}$$

By Furman et al. (2015, Eq. (6.2)), this implies bound (3.33).



## 4 An illustrative simulation study

The definition of  $\widehat{\kappa}_{m_q}^*(m, \theta, q)$  does not require observations  $(u_i, v_i)$ ,  $i \in \mathcal{M}_q$ , to arise from independent pairs  $(U_i, V_i)$ , although [Sun et al. \(2020\)](#) established consistency and other statistical properties under this assumption. Given that we are to apply the estimator on pairs arising from time series, we wish to check the estimator's robustness with respect to dependent data. The underlying time series models that are suitable for financial instruments – such as foreign currency exchange rates, stock market indices, and treasury notes – are complex: they follow, e.g., ARIMA models for the conditional mean and GARCH or some other heteroscedastic models for the conditional variance.

However, since we are concerned with co-movements of extreme losses, which are few and far between inside the original time series, the extreme losses follow models fairly close to white noise. We shall check this conjecture in [Section A.1](#) using a number of portmanteau tests. Hence, in order to check the performance of the TOMD estimator when the iid assumption is (slightly) violated, we conduct a simulated experiment when the observed pairs  $(u_i, v_i)$  arise from a time series which is not too far away from being a bivariate white noise (e.g., [Box et al., 2015](#)). Specifically, we next describe a simulation procedure for random pairs whose intra-pair dependence is governed by the generalized Clayton copula and the inter-pair dependence arises from an AR(1) time series model.

To generate  $(U_i, V_i) \sim C_{\gamma_0, \gamma_1}$ , we start with the conditional cdf of  $U$  given  $V = v$ , which has the expression

$$\mathbb{P}(U \leq u \mid V = v) = \frac{\partial}{\partial v} C_{\gamma_0, \gamma_1}(u, v) = u^{\gamma_1/\gamma^*} (u^{-1/\gamma^*} v^{1/\gamma_0} + 1 - v^{1/\gamma_0})^{-\gamma_0-1}.$$

With the notation  $z = u^{-1/\gamma^*} - 1$ , this gives

$$\begin{aligned} \mathbb{P}(U \leq (z+1)^{-\gamma^*} \mid V = v) &= (z+1)^{-\gamma_1} (zv^{1/\gamma_0} + 1)^{-\gamma_0-1} \\ &= \mathbb{P}(Y > z) \mathbb{P}(X > z \mid V = v) \\ &= \mathbb{P}(\min\{X, Y\} > z \mid V = v), \end{aligned}$$

where the random variables  $Y \sim \text{Lomax}(\gamma_1, 1)$  and  $[X \mid V = v] \sim \text{Lomax}(\gamma_0 + 1, v^{-1/\gamma_0})$  are independent. Hence, to simulate a stationary sequence  $(U_i, V_i) \sim C_{\gamma_0, \gamma_1}$ ,  $i \in \mathbb{Z}$ , we:

- (1) generate  $Z_i \sim F$  using a time series model;
- (2) set  $V_i := F(Z_i)$ ;
- (3) generate independent  $X_i \sim \text{Lomax}(\gamma_0 + 1, V_i^{-1/\gamma_0})$  and  $Y_i \sim \text{Lomax}(\gamma_1, 1)$ ;
- (4) calculate  $U_i = (1 + \min\{X_i, Y_i\})^{-\gamma^*}$ .

For step (1), we simulate  $Z_i$ 's using the strictly stationary and causal AR(1) time series

$$Z_i = \phi Z_{i-1} + \epsilon_i, \quad (\epsilon_i) \stackrel{\text{iid}}{\sim} \mathcal{N}(0, 1), \quad (4.1)$$

where  $\phi \in (-1, 1)$  regulates the departure of the sequence  $(Z_i)$  from the white noise  $(\epsilon_i)$ ; if  $\phi = 0$ , then they coincide. Since we want  $(Z_i)$  to carry some dependence, we set  $\phi = 0.6$ . Hence, the standard deviation is  $\sigma = 1/\sqrt{1 - \phi^2} = 1.25$ , and the autocovariance is  $\phi^n/(1 - \phi^2)$ ,  $n \geq 0$ .

Following steps (1)–(4), we simulate  $\{(u_i, v_i) : 1 \leq i \leq n := 500,000\}$  one thousand times, where each pair  $(u_i, v_i)$  arises from the generalized Clayton copula  $C_{\gamma_0, \gamma_1}$  with parameter choices specified in Table 4.1. The TOMD  $\kappa^*$  is calculated using formula (3.34). Table 4.1

$(\gamma_0, \gamma_1)$	$\kappa^*$	Mean	StDev	A-D	C-vM
(0.1, 0.8)	1.8	1.7920	0.0381	0.7136	0.6853
(0.4, 0.8)	1.5	1.5084	0.0221	0.6982	0.6217
(0.4, 0.2)	1.2	1.2090	0.0127	0.9758	0.9352

Table 4.1: Summary of simulation results when  $q = 0.05$ .

also contains various summary statistics under the parameter choices  $m = 5$ , which is the number of groups  $G_{j,q}$ , and  $q = 0.05$ , which is the threshold that serves our working definition of “extreme.” Note that the reported  $p$ -values of the Anderson-Darling (A-D) and Cramér-von Mises (C-vM) tests for normality retain the null hypothesis of the simulated estimator values. The fits of these values to the normal distribution are depicted in Figure 4.1. When

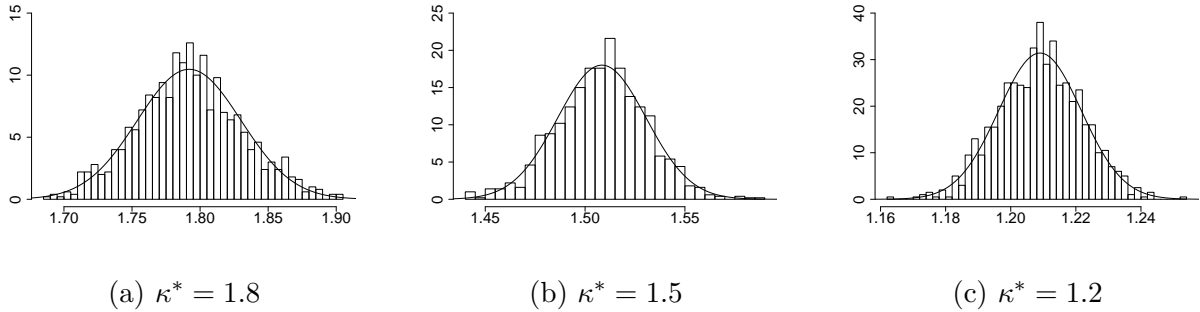


Figure 4.1: Fits of simulated  $\hat{\kappa}_{m_q}^*(5, \theta_0, 0.05)$  to the normal distribution when  $q = 0.05$ .

simulating, we always set  $\theta$  to  $\theta_0 := 10^{-6}$ .

For comparison, we use the same  $m = 5$  and parameters  $(\gamma_0, \gamma_1)$  but enlarge the threshold to  $q = 0.1$ . This increases the number of pairs in the estimated rectangle  $\mathcal{R}_q(\mathbf{0})$ . Summary

$(\gamma_0, \gamma_1)$	$\kappa^*$	Mean	StDev	A-D	C-vM
(0.1, 0.8)	1.8	1.8064	0.0197	0.9900	0.9948
(0.4, 0.8)	1.5	1.5149	0.0129	0.9807	0.9514
(0.4, 0.2)	1.2	1.2112	0.0085	0.9322	0.9373

Table 4.2: Summary of simulation results when  $q = 0.1$ .

statistics are reported in Table 4.2, with the A-D and C-vM  $p$ -values retaining the null of normality. The fits of the simulated values to the normal distribution are depicted in Figure 4.2.

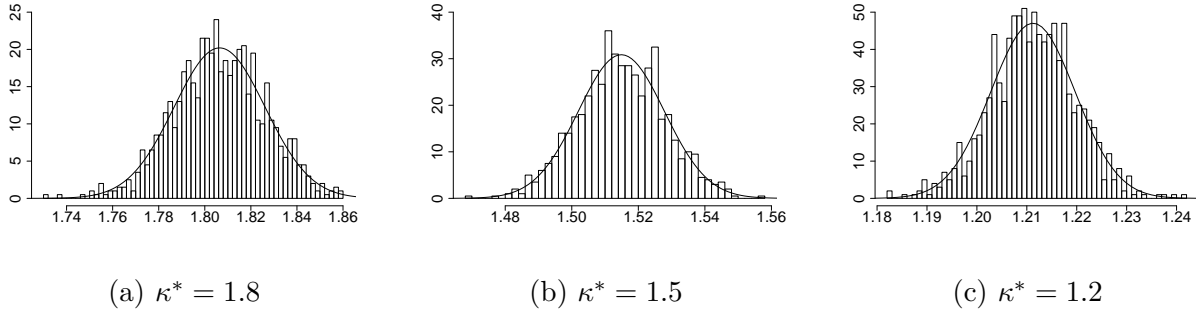


Figure 4.2: Fits of simulated  $\hat{\kappa}_{mq}^*(5, \theta_0, 0.1)$  to the normal distribution when  $q = 0.1$ .

## 5 Extreme co-movements of financial instruments

We now explore extreme co-movements of exchange rates of currencies (i.e., CAD/USD, GBP/USD, and JPY/USD), stock market indices (i.e., Dow Jones, S&P 500, and NASDAQ), and diverse financial instruments (i.e., JPY/USD, 10-year Treasury, and NASDAQ) during various periods of time, which have been determined by data availability and/or the date at which we conducted their analyses. Since several data points were missing, we removed the corresponding values from the other time series relevant to our statistical analysis. For the resulting time series  $(x_t^0)$ , we then calculated  $(x_t)$  defined by

$$x_t = \log(x_t^0) - \log(x_{t-1}^0),$$

which are depicted in the left-hand panels of Figures A.1–A.3. We have estimated the TOMD  $\kappa^*$  using the procedure described in Section 3.1. To compare, we have also estimated the TODD  $\kappa$  using the procedure described in Section 3.2. To measure the difference between the

two orders, we have calculated the relative difference in percentages:

$$\text{RD} := \left( \frac{\text{TOMD}}{\text{TODD}} - 1 \right) 100\%.$$

From the theoretical point of view, RD is always either negative or zero, but its empirical version can sometimes become positive, and we shall encounter a few such cases below.

In Figures 5.1–5.3, the upper-triangle panels depict the pairs  $(u_i/\varphi^*(q), \varphi^*(q)v_i/q^2)$ ,  $i \in \mathcal{M}_q$ , and the lower-triangle panels depict the pairs  $(u_i/q, v_i/q)$ ,  $i \in \mathcal{N}_q$ , with specially chosen thresholds  $q \in (0, 1)$  to be specified and discussed below. In all the examples, we have tested the reasonableness of the PQD assumption for paired extreme pseudo-observations  $(u_i, v_i)$  using several hypothesis tests, with findings reported in Section A.2.

## 5.1 Foreign currency exchange rates

We analyze co-movements of exchange rates of the Canadian and US dollars (CAD/USD), the pound sterling and the US dollar (GBP/USD), and the Japanese yen and the US dollar (JPY/USD) during the period from January 4, 1971, to October 25, 2019 (Federal Reserve Board, 2020). The differenced log-exchange rates  $(x_t)$  are depicted in the three left-hand panels of Figure A.1. For typographical simplicity, we abbreviate CAD/USD, GBP/USD, JPY/USD into CAD, GBP, JPY, respectively. We couple these exchange rates and analyze the strength of their co-movements in regions (determined by  $q$ ) of extreme losses. In Figure 5.1, the thresholds  $q = 0.075, 0.085$ , and  $0.1$  have been set for the pairs (JPY, CAD), (JPY, GBP), and (CAD, GBP), respectively. Their TOMD and TODD estimates are reported in Table 5.1.

JPY	1.3455	0.9026	JPY	1.2967	0.8917
123	CAD	1.5488	112	CAD	1.7759
64	57	GBP	64	53	GBP
(a) TOMD $\hat{\kappa}_{m_q}^*(5, \theta_0, q)$ and $m_q$ .			(b) TODD $\hat{\kappa}_{n_q}^{\text{OLS}}$ and $n_q$ .		

Table 5.1: The upper-triangle entries of each panel report estimated tail orders, and the lower-triangle entries report the corresponding sample sizes.

Note the relative differences:

$$\begin{aligned} (\text{JPY, CAD}) : \quad \text{RD} &= 3.76\% \\ (\text{JPY, GBP}) : \quad \text{RD} &= 1.22\% \\ (\text{CAD, GBP}) : \quad \text{RD} &= -12.79\% \end{aligned}$$

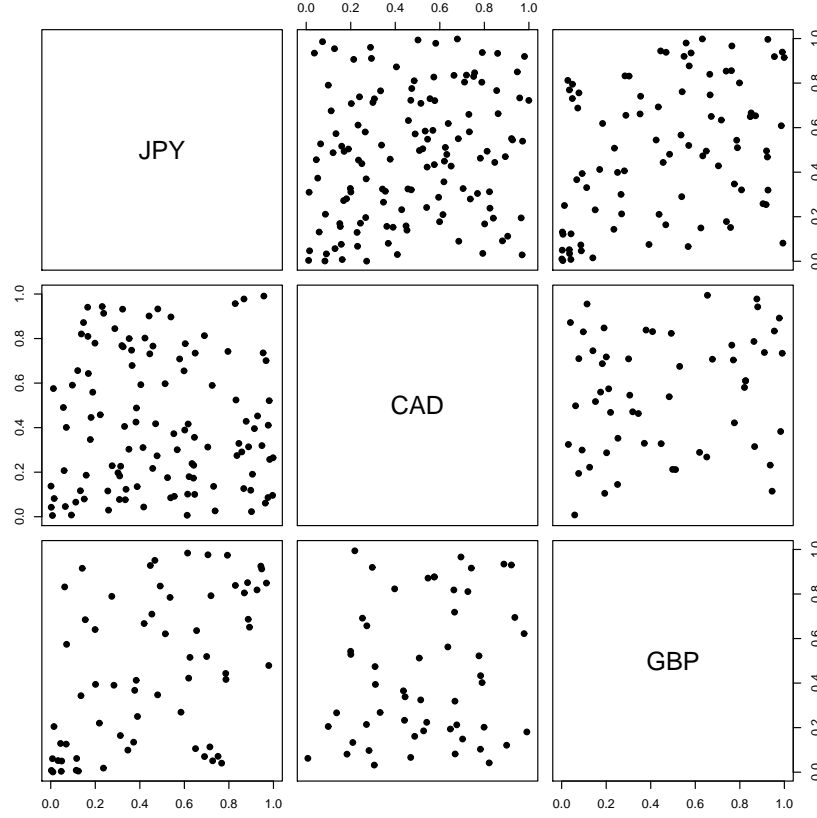


Figure 5.1: Scatterplots of pseudo observations of foreign currency exchange rates.

Although theory says that TOMD is always smaller than TODD, allowing for 5% variability makes the reported positive percentages unsurprising. We therefore conclude that (JPY, CAD) and (JPY, GBP) must have fairly similar maximal and diagonal tail orders, thus implying strong dependence within the pairs. The remaining third pair (CAD, GBP) shows an almost 13% relative decrease in the value of TOMD, thus indicating a notable increase in tail dependence when measured by TOMD if compared to TODD.

## 5.2 Stock market indices

We analyze extreme co-movements of the Dow Jones, S&P 500, and NASDAQ during the period from January 4, 1971, to February 28, 2020 ([Wall Street Journal, 2020](#); [Yahoo Finance, 2020](#)). The differenced log-time-series ( $x_t$ ) are depicted in the three left-hand panels of Figure A.2. We pair these time series and analyze the strength of their co-movements in regions of extreme losses. In Figure 5.2, the thresholds  $q = 0.0075$ ,  $0.01$ , and  $0.0075$  have been set for the pairs (Dow Jones, S&P 500), (Dow Jones, NASDAQ), and (S&P 500, NASDAQ),

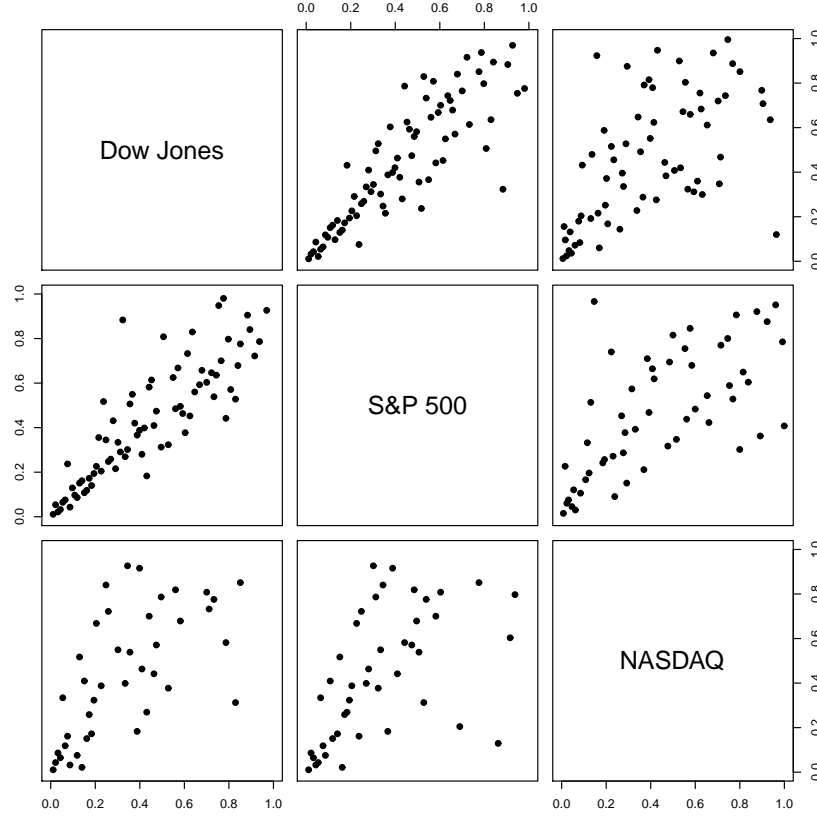


Figure 5.2: Scatterplots of pseudo observations of stock market indices.

respectively. Their TOMD and TODD estimates are reported in Table 5.2. Note the relative

Dow Jones	0.8329	0.9816	Dow Jones	1.0788	0.9874
77	S&P 500	0.9422	77	S&P 500	0.9710
68	53	NASDAQ	61	44	NASDAQ
(a) TOMD $\hat{\kappa}_{m_q}^*(5, \theta_0, q)$ and $m_q$ .			(b) TODD $\hat{\kappa}_{n_q}^{\text{OLS}}$ and $n_q$ .		

Table 5.2: The upper-triangle entries of each panel report estimated tail orders, and the lower-triangle entries report the corresponding sample sizes.

differences:

$$\begin{aligned}
 (\text{Dow Jones, S\&P 500}) : \quad \text{RD} &= -22.79\% \\
 (\text{Dow Jones, NASDAQ}) : \quad \text{RD} &= -0.59\% \\
 (\text{S\&P 500, NASDAQ}) : \quad \text{RD} &= -2.97\%
 \end{aligned}$$

All the values of TOMD are smaller than the corresponding ones of TODD. The pair (Dow Jones, S&P 500) shows an almost 23% decrease in the value of TOMD if compared to the diagonal case, and thus increase in tail dependence when measured by TOMD. Allowing for 5% variability, we conclude that (Dow Jones, NASDAQ) and (S&P 500, NASDAQ) have quite similar TOMD and TODD, thus implying strong dependence within the pairs.

### 5.3 Diverse financial instruments

We analyze pairwise extreme co-movements between daily returns of three different financial instruments: JPY/USD ([Federal Reserve Board, 2020](#)), US 10-year Treasury shorthand as US10YT, and NASDAQ ([Yahoo Finance, 2020](#)), which belong to the categories of exchange rates, treasury notes, and stock market indices, respectively. The historical data are from February 5, 1971, to March 3, 2020. The differenced log-time-series ( $x_t$ ) are depicted in the three left-hand panels of Figure A.3. We pair these time series and analyze the strength of their co-movements in regions of extreme losses. In Figure 5.3, the thresholds  $q = 0.05$ ,

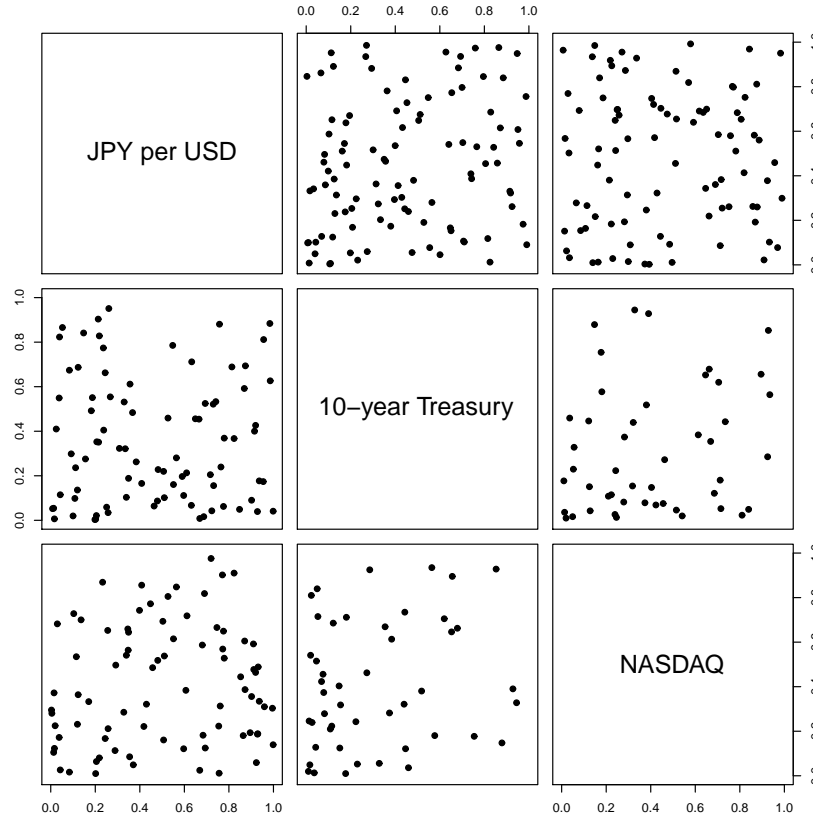


Figure 5.3: The pseudo observations under consideration of diverse financial instruments.

0.05, and 0.025 have been set for the pairs (JPY/USD, US10YT), (JPY/USD, NASDAQ), and (US10YT, NASDAQ), respectively. Their TOMD and TODD estimates are reported in

JPY/USD	1.1648	1.4002	JPY/USD	1.3146	1.5276
89	US10YT	0.8516	85	US10YT	1.1292
87	47	NASDAQ	80	47	NASDAQ

(a) TOMD  $\hat{\kappa}_{m_q}^*(5, \theta_0, q)$  and  $m_q$ .

(b) TODD  $\hat{\kappa}_{n_q}^{\text{OLS}}$  and  $n_q$ .

Table 5.3: The upper-triangle entries of each panel report estimated tail orders, and the lower-triangle entries report the corresponding sample sizes.

Table 5.3. Note the relative differences:

$$\begin{aligned}
(\text{JPY/USD, US10YT}) : \quad \text{RD} &= -11.40\% \\
(\text{JPY/USD, NASDAQ}) : \quad \text{RD} &= -8.34\% \\
(\text{US10YT, NASDAQ}) : \quad \text{RD} &= -24.58\%
\end{aligned}$$

All the values of TOMD are smaller than the corresponding ones of TODD, and all the pairs show considerable decrease in the values of TOMD if compared to the diagonal case.

## 6 Conclusion

In this paper we have developed a substantial extension of the procedure of [Sun et al. \(2020\)](#) for assessing the maximal strength of co-movements of extreme losses when original data follow dependent dynamical models. We have explored the performance of the modification on simulated bivariate time series. The study has shown that the block-wise construction of the estimator of maximal tail dependence successfully handles time series structures of data sets and, in turn, from them arising extreme co-movements. The validity of underlying theoretical assumptions has been tested using appropriate statistical tests, and the calculation of critical values has been discussed. In addition, we have provided an extensive study of thresholds below which time-series data give rise to what we deem to be extreme losses. The strength of maximal dependence as well as of the classical diagonal dependence have been explored and compared for a number of positively quadrant dependent financial instruments, such as foreign exchange rates of several major currencies, stock market indices, and treasury notes.



## References

- Ahsanullah, M., Nevzorov, V.B. and Shakil, M. (2013). *An Introduction to Order Statistics*. Atlantis Press, Paris.
- Arnold, B.C., Balakrishnan, N. and Nagaraja, H.N. (2008). *A First Course in Order Statistics*. Society for Industrial and Applied Mathematics, Philadelphia.
- Bojanic, R. and Seneta, E. (1971). Slowly varying functions and asymptotic relations. *Journal of Mathematical Analysis and Applications*, 34, 302–315.
- Box, G.E.P., Jenkins, G.M., Reinsel, G.C. and Ljung, G.M. (2015). *Time Series Analysis: Forecasting and Control*. (Fifth edition.) Wiley, New York.
- Box, G.E.P. and Pierce, D.A. (1970). Distribution of residual autocorrelation in autoregressive integrated moving average time series models. *Journal of American Statistical Association*, 65, 1509–1526.
- Bücher, A., Jäschke, S., and Wied, D. (2015). Nonparametric tests for constant tail dependence with an application to energy and finance. *Journal of Econometrics*, 187, 154–168.
- Calabrese, R., and Osmetti, S.A. (2014). Modelling cross-border systemic risk in the European banking sector: a copula approach. *Technical Report*, arXiv:1411.1348, 1–19.
- Castillo, E., Hadi, A.S., Balakrishnan, N. and Sarabia, J.M. (2004). *Extreme Value and Related Models with Applications in Engineering and Science*. Wiley, New York.
- Cherubini, U., Luciano, E., and Vecchiato, W. (2013). *Copula Methods in Finance*. Wiley, New York.
- David, H.A. and Nagaraja, H.N. (2003). *Order Statistics*. (Third Edition.) Wiley, Hoboken.
- Davydov, Y. and Zitikis, R. (2008). On weak convergence of random fields. *Annals of the Institute of Statistical Mathematics*, 60, 345–365.
- Durante, F., Pappadà, R., and Torelli, N. (2014). Clustering of financial time series in risky scenarios. *Advances in Data Analysis and Classification*, 8, 359–376.
- Federal Reserve Board (2020). *Foreign Exchange Rates – H.10*. Board of Governors of the Federal Reserve System, Washington, D.C. <https://www.federalreserve.gov/releases/h10/>
- Frahm, G., Junker, M., and Schmidt, R. (2005). Estimating the tail-dependence coefficient: properties and pitfalls. *Insurance: Mathematics and Economics*, 37, 80–100.
- Furman, E., Kuznetsov, A., Su, J., and Zitikis, R. (2016). Tail dependence of the Gaussian copula revisited. *Insurance: Mathematics and Economics*, 69, 97–103.
- Furman, E., Su, J., and Zitikis, R. (2015). Paths and indices of maximal tail dependence.

- ASTIN Bulletin: the Journal of the International Actuarial Association*, 45, 661–678.
- Gabaix, X., and Ibragimov, R. (2011). Rank-1/2: a simple way to improve the OLS estimation of tail exponents. *Journal of Business and Economic Statistics*, 29, 24–39.
- Hosking, J.R.M. (1980). The multivariate portmanteau statistic. *Journal of American Statistical Association*, 75, 602–608.
- Kiefer, J. (1961). On large deviations of the empiric D. F. of vector chance variables and a law of the iterated logarithm. *Pacific Journal of Mathematics*, 11, 649–660.
- Kiefer, J. and Wolfowitz, J. (1958). On the deviations of the empiric distribution function of vector chance variables. *Transactions of the American Mathematical Society*, 87, 173–186.
- Kontorovich, A. and Weiss, R. (2014). Uniform Chernoff and Dvoretzky-Kiefer-Wolfowitz-type inequalities for Markov chains and related processes. *Journal of Applied Probability*, 51, 1100–1113.
- Li, W.K. and McLeod, A.I. (1981). Distribution of the residual autocorrelations in multivariate ARMA time series models. *Journal of the Royal Statistical Society, Series B*, 43, 231–239.
- Liu, X., Wu, J., Yang, C., and Jiang, W. (2018). A maximal tail dependence-based clustering procedure for financial time series and its applications in portfolio selection. *Risks*, 6, 1–26 (Article #115).
- Ljung, G.M. and Box, G.E.P (1978). On a measure of lack of fit in time series models. *Biometrika*, 65, 297–303.
- Mahdi, E. and McLeod, A.I. (2012). Improved multivariate portmanteau test. *Journal of Time Series Analysis*, 33, 211–222.
- Nelsen, R.B., Quesada-Molina, J.J., Rodríguez-Lallena, J.A., and Úbeda-Flores, M. (2003). Kendall distribution functions. *Statistics and Probability Letters*, 65, 263–268.
- Pericoli, M., and Sbracia, M. (2003). A primer on financial contagion. *Journal of Economic Surveys*, 17, 571–608.
- Sun, N., Yang, C., and Zitikis, R. (2020). A statistical methodology for assessing the maximal strength of tail dependence. *ASTIN Bulletin: the Journal of the International Actuarial Association* 50, 799–825.
- Tang, C.F., Wang, D., El Barmi, H. and Tebbs, J.M. (2019). Testing for positive quadrant dependence. *American Statistician*, 30, 1–15.
- Wall Street Journal (2020). Market data: Dow Jones Industrial Average. <https://www.wsj.com/market-data/quotes/index/DJIA/historical-prices>
- White, H., Kim, T.-H., Manganelli, S. (2015). VAR for VaR: measuring tail dependence using

multivariate regression quantiles. *Journal of Econometrics*, 187, 169–188.

Yahoo Finance (2020). Market data. <https://ca.finance.yahoo.com/>

## A Appendix

### A.1 Thresholds and pseudo observations

In Figures A.1–A.3 we have depicted the differenced log-time-series  $x_t = \log(x_t^0) - \log(x_{t-1}^0)$  (left-hand panels) and the extreme pseudo-observations (right-hand panels) that arise from the time series data specified in Section 5.

With thresholds  $q \in (0, 1)$  reported in Table A.1, the time series give rise to paired extreme

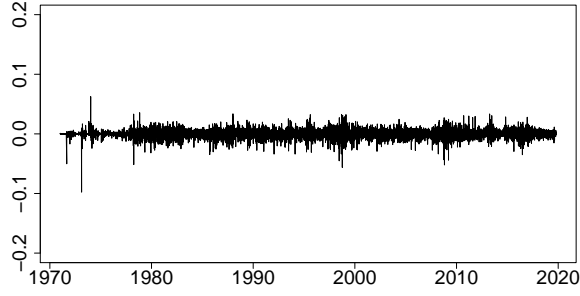
Pairs	Threshold $q$						
	0.0075	0.01	0.025	0.05	0.075	0.085	0.1
(JPY, CAD)	...	...	...	...	100(123)	...	...
(JPY, GBP)	...	...	...	...	...	90(64)	...
(CAD, GBP)	...	...	...	...	...	...	95(57)
(Dow Jones, S&P 500)	60(77)	...	...	...	...	...	...
(Dow Jones, NASDAQ)	...	77(68)	...	...	...	...	...
(S&P 500, NASDAQ)	76(53)	...	...	...	...	...	...
(JPY/USD, US10YT)	...	...	...	100(89)	...	...	...
(JPY/USD, NASDAQ)	...	...	...	100(87)	...	...	...
(US10YT, NASDAQ)	...	...	88(47)	...	...	...	...

Table A.1: The percentages of  $p$ -values retaining the null of white noise at the significance level  $\alpha = 0.05$  alongside the sample sizes  $m_q$  (in parentheses) for appropriate choices of  $q$ .

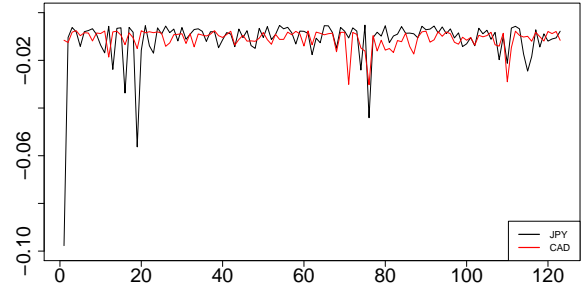
pseudo-observations that resemble white noise; see the right-hand panels of Figures A.1–A.3. To substantiate this claim, we have run several portmanteau tests for the null hypothesis

$$\mathcal{H}_0 : \mathbf{\Gamma}_L = \mathbf{0}, \quad L = 1, \dots, 20,$$

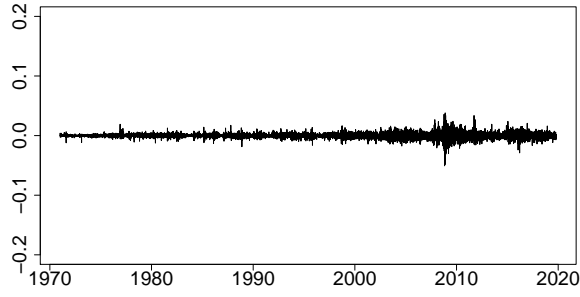
where  $\mathbf{\Gamma}_L = \text{Cov}(\boldsymbol{\varepsilon}_t, \boldsymbol{\varepsilon}_{t-L})$  and  $(\boldsymbol{\varepsilon}_t)_{t=1}^{m_q}$  are the residuals obtained by fitting the original data to the time series model VARMA for sufficiently many lags (Mahdi and McLeod, 2012). The selected portmanteau tests include those of Mahdi and McLeod (2012), Box and Pierce (1970),



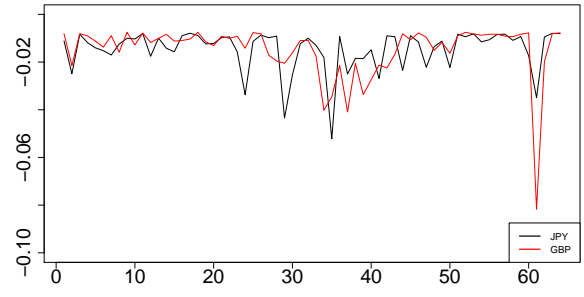
(a) JPY/USD



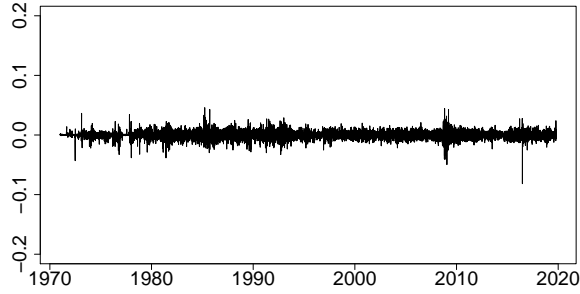
(b) (JPY, CAD),  $q = 0.075$ ,  $m_q = 123$ .



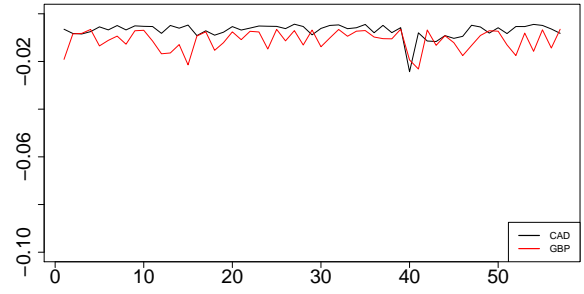
(c) CAD/USD



(d) (JPY, GBP),  $q = 0.085$ ,  $m_q = 64$ .



(e) GBP/USD

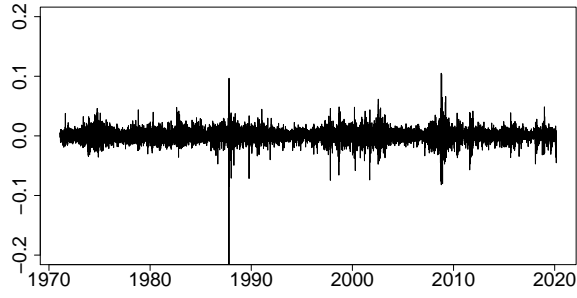


(f) (CAD, GBP),  $q = 0.1$ ,  $m_q = 57$ .

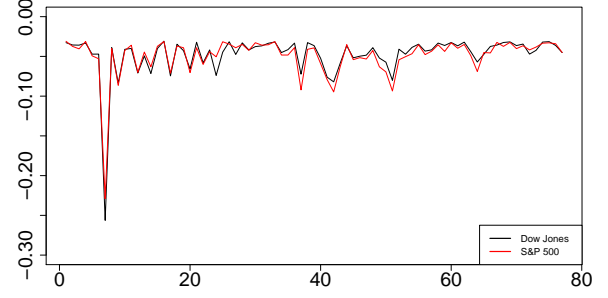
Figure A.1: Original  $x_t$ 's (left-hand panels) and the pairs of extreme pseudo-observations (right-hand panels) for foreign currency exchange from January 4, 1971, to October 25, 2019.

Ljung and Box (1978), Hosking (1980), and Li and McLeod (1981). The percentages of  $p$ -values above the 5% significance level (meaning that the null of white noise is retained) are reported in Table A.1, where we also report the sample sizes  $m_q$ .

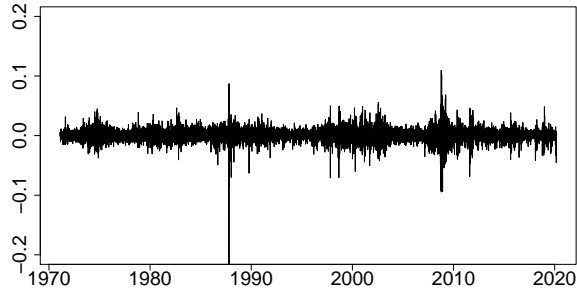
The different choices of  $q \in (0, 1)$  warrant an explanation. First, we want to work with as small  $q > 0$  as possible, mainly due to two reasons: the estimator's deterministic bias



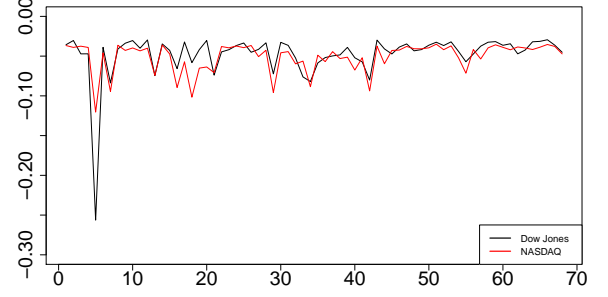
(a) Dow Jones



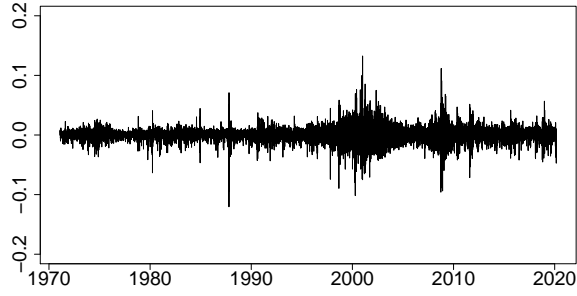
(b) (Dow Jones, S&P 500),  $q = 0.0075$ ,  $m_q = 77$ .



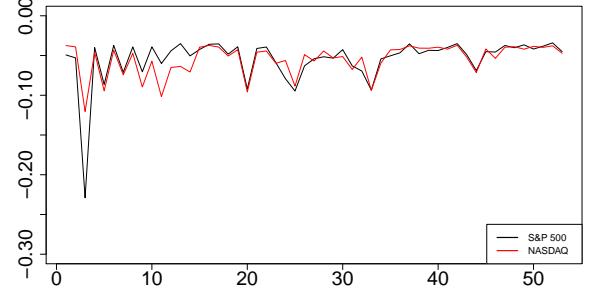
(c) S&P 500



(d) (Dow Jones, NASDAQ),  $q = 0.01$ ,  $m_q = 68$ .



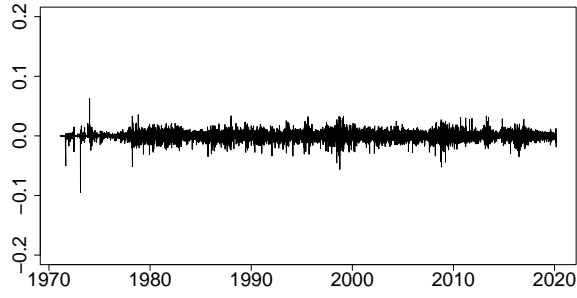
(e) NASDAQ



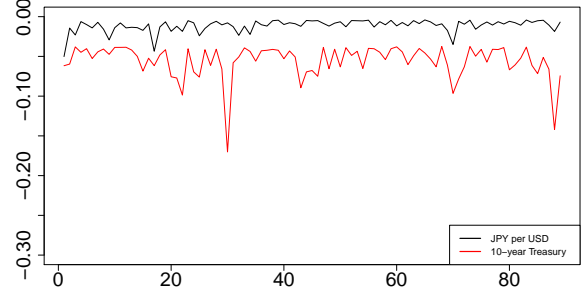
(f) (S&P 500, NASDAQ),  $q = 0.0075$ ,  $m_q = 53$ .

Figure A.2: Original  $x_t$ 's (left-hand panels) and the pairs of extreme pseudo-observations (right-hand panels) for stock market indices from January 4, 1971, to February 28, 2020.

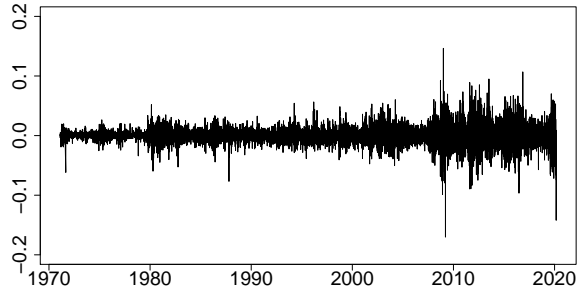
becomes small (recall Theorem 3.1), and the two-dimensional time series of extreme pseudo-observations becomes nearly white-noise. Working close to white noise is important in order to reliably calculate critical values of the PQD tests, which verify the applicability of Theorem 3.1.



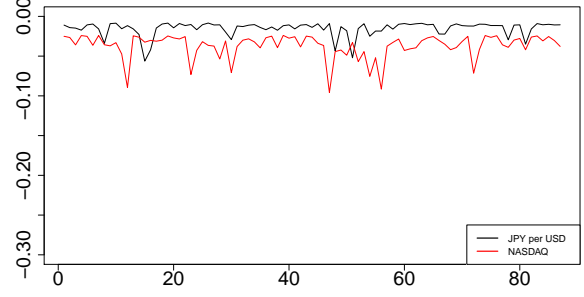
(a) JPY/USD



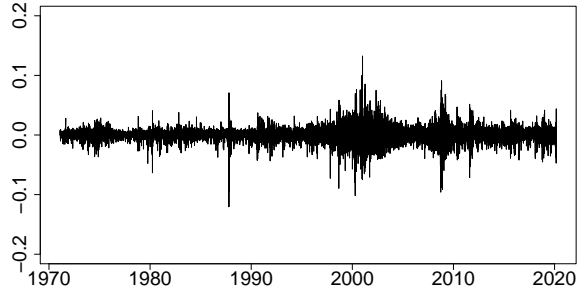
(b) (JPY/USD, US10YT),  $q = 0.05$ ,  $m_q = 89$ .



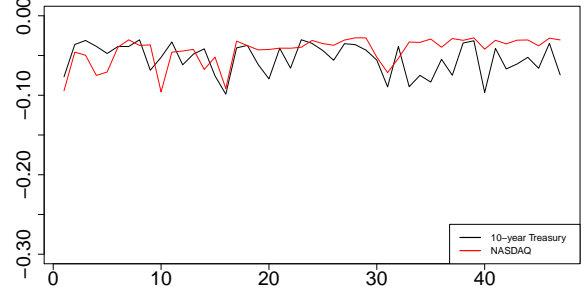
(c) US10YT



(d) (JPY/USD, NASDAQ),  $q = 0.05$ ,  $m_q = 87$ .



(e) NASDAQ



(f) (US10YT, NASDAQ),  $q = 0.025$ ,  $m_q = 47$ .

Figure A.3: Original  $x_t$ 's (left-hand panels) and the pairs of extreme pseudo-observations (right-hand panels) for diverse financial instruments from February 5, 1971, to March 3, 2020.

## A.2 Testing PQD vs. not PQD

In all the real time-series examples that we explore, we statistically test the reasonableness of the PQD assumption for the cdf  $F_q^*$  defined in equation (3.5). For this, we use the Kolmogorov-Smirnov (K-S), Cramér-von Mises (C-vM), Anderson-Darling (A-D) one-sided statistics (e.g.,

Tang et al., 2019, and references therein):

$$\sqrt{m_q} \sup_{(u,v) \in [0,1]^2} \{uv - F_{q,\mathcal{M}_q}^*(u,v)\}_+, \quad (\text{A.1})$$

$$m_q \int_{[0,1]^2} (\{uv - F_{q,\mathcal{M}_q}^*(u,v)\}_+)^2 dF_{q,\mathcal{M}_q}^*(u,v), \quad (\text{A.2})$$

$$m_q \int_{[0,1]^2} \frac{(\{uv - F_{q,\mathcal{M}_q}^*(u,v)\}_+)^2}{u(1-u)v(1-v)} dF_{q,\mathcal{M}_q}^*(u,v), \quad (\text{A.3})$$

respectively, where  $F_{q,\mathcal{M}_q}^*$  is defined in equation (3.6). Specifically, we use these statistics to test the null of PQD versus the alternative of not PQD:

$$\text{PQD: } F_q^*(u,v) \geq uv \text{ for all } (u,v) \in [0,1]^2$$

$$\text{Not PQD: } F_q^*(u,v) < uv \text{ for some } (u,v) \in [0,1]^2$$

The critical values of these tests are obtained by sampling from the pairs of pseudo observations. Namely, we calculate the test statistics, repeat the procedure  $N = 10,000$  times obtain so many values of the test statistics, and finally calculate the 95th percentiles of the respective test-statistic values. The decision rule is to retain the null hypothesis of PQD if the test statistic is smaller than the critical value, and to reject it otherwise. The obtained results are summarized in Tables A.2–A.4, where the abbreviations “Stat,” “Crit,” and “Deci” stand for the test statistic value, the critical value, and the decision, respectively. The decision is to

	(JPY, CAD)			(JPY, GBP)			(CAD, GBP)		
	$q = 0.075, m_q = 123$			$q = 0.085, m_q = 64$			$q = 0.1, m_q = 57$		
Test	Stat	Crit	Deci	Stat	Crit	Deci	Stat	Crit	Deci
K-S	0.0189	1.2119	PQD	0.0404	1.1195	PQD	0.5781	1.0989	PQD
C-vM	0.0000	0.2013	PQD	0.0000	0.1844	PQD	0.0330	0.1737	PQD
A-D	0.0008	28.7139	PQD	0.0064	23.9732	PQD	6.0110	24.5422	PQD

Table A.2: Testing PQD vs not PQD of pseudo observations of foreign currency exchange rates.

retain the null of PQD when the statistic is smaller than the critical value. In every case, the three tests have retained the null of PQD. To gain additional insight, in next Section A.3 we also test the null of independence, which is a “boundary” case for PQD, versus the alternative of strict PQD.

	(Dow Jones, S&P 500)			(Dow Jones, NASDAQ)			(S&P 500, NASDAQ)		
	$q = 0.0075, m_q = 77$			$q = 0.01, m_q = 68$			$q = 0.0075, m_q = 53$		
Test	Stat	Crit	Deci	Stat	Crit	Deci	Stat	Crit	Deci
K-S	0.0000	1.1474	PQD	0.0000	1.1350	PQD	0.0000	1.0905	PQD
C-vM	0.0000	0.1922	PQD	0.0000	0.1900	PQD	0.0000	0.1786	PQD
A-D	0.0000	26.5523	PQD	0.0000	24.7340	PQD	0.0000	22.9812	PQD

Table A.3: Testing PQD vs not PQD of pseudo observations of stock market indices.

	(JPY/USD, US10YT)			(JPY/USD, NASDAQ)			(US10YT, NASDAQ)		
	$q = 0.05, m_q = 89$			$q = 0.05, m_q = 87$			$q = 0.025, m_q = 47$		
Test	Stat	Crit	Deci	Stat	Crit	Deci	Stat	Crit	Deci
K-S	0.0000	1.1715	PQD	0.1913	1.1766	PQD	0.0000	1.0739	PQD
C-vM	0.0000	0.1889	PQD	0.0007	0.2004	PQD	0.0000	0.1794	PQD
A-D	0.0000	25.2966	PQD	0.6637	26.5172	PQD	0.0000	23.8698	PQD

Table A.4: Testing PQD vs not PQD of pseudo observations of diverse financial instruments.

### A.3 Testing independence vs. strict PQD

In the examples of Section A.2, all of which retained the null of PQD for the cdf  $F_q^*$ , we now statistically test the reasonableness of independence versus strict PQD, the latter shorthanded as SPQD. We use the Kolmogorov-Smirnov (K-S), Cramér-von Mises (C-vM), Anderson-Darling (A-D) one-sided statistics (cf. Tang et al., 2019):

$$\sqrt{m_q} \sup_{(u,v) \in [0,1]^2} \{F_{q,\mathcal{M}_q}^*(u,v) - uv\}_+, \quad (\text{A.4})$$

$$m_q \int_{[0,1]^2} (\{F_{q,\mathcal{M}_q}^*(u,v) - uv\}_+)^2 dF_{q,\mathcal{M}_q}^*(u,v), \quad (\text{A.5})$$

$$m_q \int_{[0,1]^2} \frac{(\{F_{q,\mathcal{M}_q}^*(u,v) - uv\}_+)^2}{u(1-u)v(1-v)} dF_{q,\mathcal{M}_q}^*(u,v), \quad (\text{A.6})$$

respectively. Specifically, we use statistics (A.4)–(A.6) to test the null of independence (IND) versus the alternative of strict PQD:

$$\text{IND: } F_q^*(u,v) = uv \text{ for all } (u,v) \in [0,1]^2$$

$$\text{SPQD: } F_q^*(u,v) > uv \text{ for some } (u,v) \in [0,1]^2$$



The procedure for calculating the critical values is analogous to that used in Section A.2, and the decision to retain the null of independence (IND) is taken when the statistic is smaller than the critical value. Our findings are summarized in Tables A.5–A.6.

	(JPY, CAD)			(JPY, GBP)			(CAD, GBP)		
	$q = 0.075, m_q = 123$			$q = 0.085, m_q = 64$			$q = 0.1, m_q = 57$		
Test	Stat	Crit	Deci	Stat	Crit	Deci	Stat	Crit	Deci
K-S	1.4859	1.3546	SPQD	1.4837	1.3386	SPQD	0.9139	1.3231	IND
C-vM	0.5874	0.2969	SPQD	0.6968	0.3198	SPQD	0.0782	0.3299	IND
A-D	25.6607	44.9833	IND	91.2540	50.1569	SPQD	4.0293	49.6459	IND

Table A.5: Testing IND vs SPQD of pseudo observations of foreign currency exchange rates.

	(Dow Jones, S&P 500)			(Dow Jones, NASDAQ)			(S&P 500, NASDAQ)		
	$q = 0.0075, m_q = 77$			$q = 0.01, m_q = 68$			$q = 0.0075, m_q = 53$		
Test	Stat	Crit	Deci	Stat	Crit	Deci	Stat	Crit	Deci
K-S	2.4058	1.3441	SPQD	1.7760	1.3335	SPQD	1.6858	1.3208	SPQD
C-vM	2.9460	0.3107	SPQD	1.3744	0.3269	SPQD	1.3100	0.3343	SPQD
A-D	90.9184	47.4610	SPQD	61.2180	49.3820	SPQD	51.2729	51.2274	SPQD

Table A.6: Testing IND vs SPQD of pseudo observations of stock market indices.

	(JPY/USD, US10YT)			(JPY/USD, NASDAQ)			(US10YT, NASDAQ)		
	$q = 0.05, m_q = 89$			$q = 0.05, m_q = 87$			$q = 0.025, m_q = 47$		
Test	Stat	Crit	Deci	Stat	Crit	Deci	Stat	Crit	Deci
K-S	1.8927	1.3442	SPQD	0.8564	1.3465	IND	2.1463	1.3158	SPQD
C-vM	1.0709	0.3092	SPQD	0.2266	0.3142	IND	1.4086	0.3345	SPQD
A-D	79.7641	49.0677	SPQD	33.5631	48.3546	IND	71.3135	52.2009	SPQD

Table A.7: Testing IND vs SPQD of pseudo observations of diverse financial instruments.